WADC TECHNICAL REPORT 52-171

ANALYSIS OF MAGNETRON OSCILLATIONS AT LOW MAGNETIC AND ELECTRIC FIELDS

JOHN L. MOLL

OHIO STATE UNIVERSITY RESEARCH FOUNDATION

JUNE 1952

WRIGHT AIR DEVELOPMENT CENTER
Air Research and Development Command
United States Air Force
Wright-Patterson Air Force Base, Ohio

I

WADC TECHNICAL REPORT 52-171

ANALYSIS OF MAGNETRON OSCILLATIONS AT LOW MAGNETIC AND ELECTRIC FIELDS

JOHN L. MOLL

June 1952

Ohio State University Research Foundation
Air Force Contract No. W33-038-ac-15162
RDO No. R-111-51

Wright Air Development Center
Air Research and Development Command
United States Air Force
Wright-Patterson Air Force Base, Ohio

II

GOVERNMENT NOTICES

When Government drawings, specifications or other data are used for any purpose other than in connection with a definitely related Government procurement operation, the United States Government thereby incurs no responsibility nor any obligation whatsoever; and the fact that the Government may have formulated, furnished, or in any way supplied the said drawings, specifications, or other data, is not to be regarded by implication or otherwise as in any manner licensing the holder or any other person or corporation, or conveying any rights or permission to manufacture, use, or sell any patented invention that may in any way be related thereto.

The information furnished herewith is made available for study upon the understanding that the Government's proprietary interests in and relating thereto shall not be impaired. It is desired that the Judge Advocate Office, WCJ, Wright Air Development Center, Wright-Patterson Air Force Base, Ohio, be promptly notified of any apparent conflict between the Government's proprietary interests and those of others.

FOREWORD

The information contained in this report was originally presented as a dissertation in partial fulfillment of the requirements for the Degree Doctor of Philosophy in the Graduate School of The Ohio State University.

The work described in the dissertation was done at the Electron Tube Laboratory of the Department of Electrical Engineering, The Ohio State University, and was directed and approved by E. M. Boone, Research Supervisor, under Air Force Contract W33-038-ac-15162, Research and Development Order No. R-111-51, "Wide Range Tuning Klystrons." It was administered under the direction of the Components and Systems Laboratory, Wright Air Development Center, with Mr. Ludwig Mayer acting as project engineer.

Acknowledgements should be made to Mr. E. E. Willshaw of G. E. C. of England who first made the possibility of low field magnetron operation seem practical (see ref. 3). Mr. R. L. Walters, D. Wolking and J. Peck of the Electron Tube Laboratory performed most of the experiments. Professor E. M. Boone gave many valuable criticisms of the dissertation.

ABSTRACT

Research was undertaken to investigate the possibility of operating a multicavity magnetron at values of electrical and magnetic field near the characteristic values. This would make possible the scaling of the magnetron to very short wavelengths before encountering difficulties with anode heating and magnetic field limitations. The essential change in design for low field operation is the use of a small cathode diameter.

An account is given of a familiar theoretical concept of ordinary magnetron operation and this is related to the operation at low fields. Electron trajectories are calculated for low field conditions. The theoretical concept of low field operation is in general agreement with experimental results obtained at this laboratory.

Experimental results are given for an 18 segment anode. It is essential that a sharp cut-off curve be obtained to allow for low field oscillations. The violation of the Hull cut-off relation at high voltage places a limitation on the voltage at which it is possible to design low field magnetrons.

PUBLICATION REVIEW

The publication of this report does not constitute approval by the Air Force of the findings or the conclusions contained therein. It is published only for the exchange and stimulation of ideas.

FOR THE COMMANDING GENERAL:

DANIEL B. WHITE
Colonel, USAF
Chief, Weapons Components Division

TABLE OF CONTENTS

VI

LIST OF ILLUSTRATIONS

ANALYSIS OF MAGNETRON OSCILLATIONS AT LOW MAGNETIC AND ELECTRIC FIELDS

Magnetron Types

Magnetrons have been used for many years to generate very high frequencies. As the demand for higher frequencies continued, newer types of magnetrons were developed to satisfy the requirements of high power generators. During World War II, the traveling wave type or multi-cavity magnetron was developed to a high degree as a pulsed generator for radar transmitters and as a high power C.W. oscillator. Figure 1 illustrates in schematic outline a modern traveling wave type oscillator.

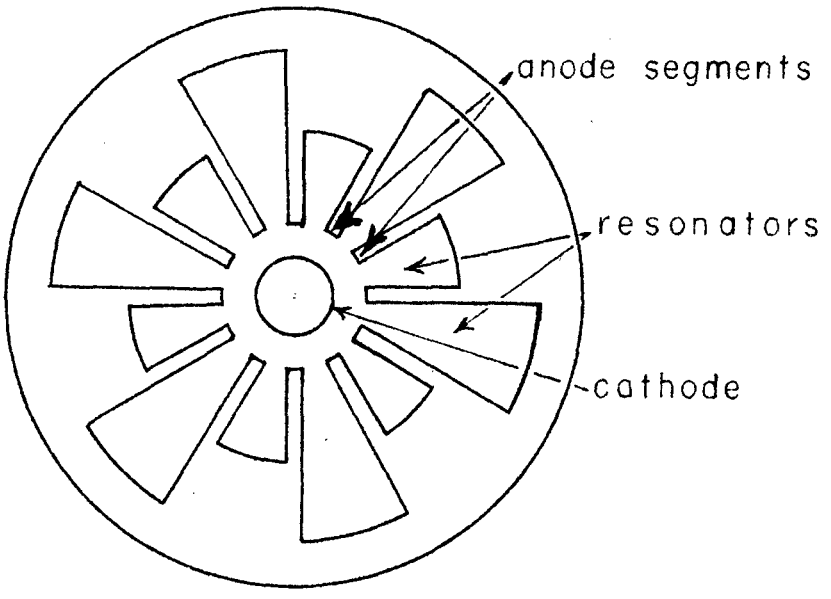

Figure 1.
Magnetron outline showing rising sun type resonant circuit.

Before discussing the electronic behavior of magnetrons, a word should be said concerning the resonant circuit. Successful resonant

circuits for centimeter wave magnetrons fall into three general classes: rising sun, strapped anodes and interdigital resonators. It is usual to design the magnetron resonator to operate in the π-mode, or resonant mode, in which there is 180° phase shift from one anode segment to the next. Since the magnetron resonator has many resonant modes, it is necessary to suppress the undesired ones, or move their resonant frequencies away from the π-mode. It is not the purpose of this paper to discuss the way in which this is accomplished. However, Figure 2 illustrates the three types of resonators which have successfully accomplished this purpose. The rising sun type was used in the experimental work (to be described in later pages) since this type of anode is easiest to fabricate. Except for minor differences, the electronic behavior is the same for the different types of anodes.[1], [2]

It is the purpose of this report to discuss the electronic behavior of magnetrons at relatively lower magnetic fields and voltages than are used in the conventional type operation of an oscillator of the same size.[3]

Traveling Wave Type Magnetron

In order to make clear some of the contrasts in the behavior of magnetrons at low fields, it will be necessary to point out some of the characteristics of ordinary traveling wave magnetrons. A discussion of what happens in the magnetron interaction space (the space

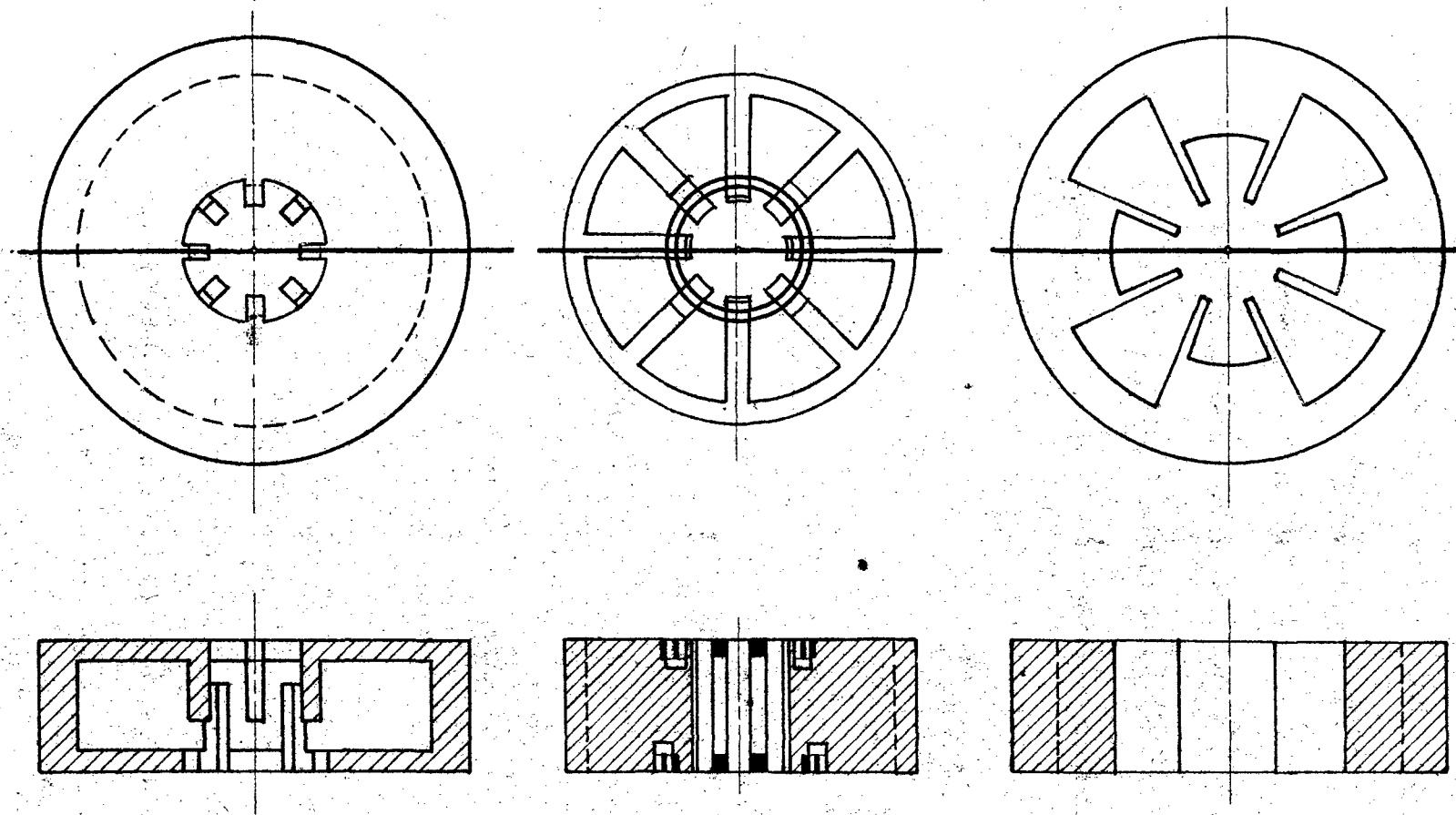

Figure 2.

Resonant circuits for magnetrons.

between cathode and anode segments) is most easily based on the equations of motion and Maxwell's equations.

For the discussion of the electronic interaction, non-relativistic mechanics will be assumed. Also, the effect of the magnetic field associated with the alternating electric field will be neglected. Appendix II discusses the magnitude of the relativistic effects for planar and cylindrical geometry. Planar and cylindrical inverted (i.e., cathode on outside, anode segments on the inside) magnetrons have been successfully operated, but the principal interest in this paper will be the ordinary type interaction space, in which a cylindrical cathode is surrounded by a cylindrical anode, as in Figure 1. End effects will be neglected, and it is assumed that the anode current, power input and output of the magnetron are proportional to its length. With these assumptions, it is seen that the static electrical field is radial. For convenience of analysis, π-mode operation will be assumed. It would be possible to keep a generalized notation, but this would only complicate the algebra, and would not contribute to the generality of the results. In the π-mode of resonance, the instantaneous angular electric field at the anode radius is as shown in Figure 3. The letter ϕ is used for angle. Cylindrical coordinates are used, and the magnetic field is in the axial or z-direction.

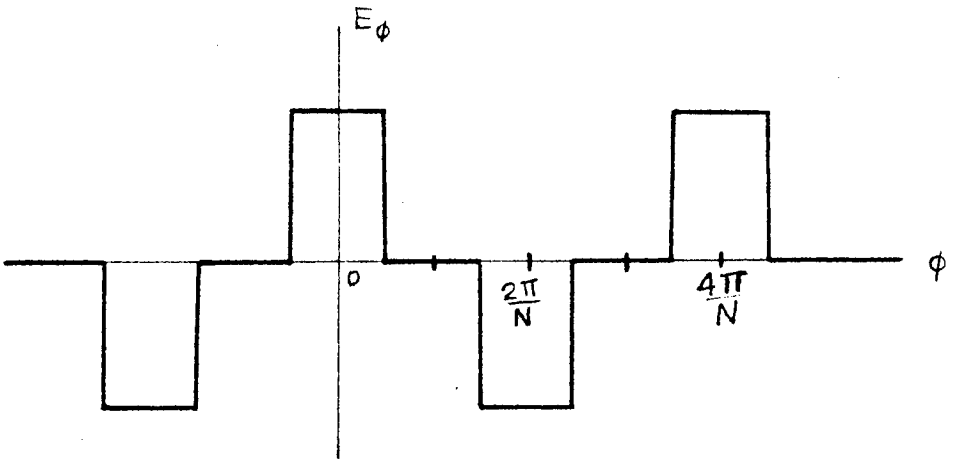

Figure 3.

Electric field at magnetron anode.

The electric field is zero at the tip of the anode segment or vane, and alternately positive and negative at the succeeding gaps. At the cathode, the angular field is zero. If it is assumed that all alternating fields vary as $e^{j\omega t}$ (real part being understood), then the following relationships are obtained from Maxwell's equations:

$$\bar{E}_r = \frac{1}{j\omega \epsilon r} \frac{\partial \bar{H}_z}{\partial \phi} \tag{1}$$

$$\bar{E}_\phi = - \frac{1}{j\omega \epsilon} \frac{\partial \bar{H}_z}{\partial r} , \tag{2}$$

$$\frac{1}{r} \frac{\partial}{\partial r} \left(r \frac{\partial \bar{H}_z}{\partial r} \right) + \frac{1}{r^2} \frac{\partial^2 \bar{H}_z}{\partial \phi^2} + \omega^2 \mu \epsilon \bar{H}_z = 0 \tag{3}$$

where $\overline{E}_r$, $\overline{E}_\phi$ and $\overline{H}_z$ are functions of r and ϕ only but not functions of t. This formulation neglects the effect of space charge on the rf field configuration. Equation (3) has solutions of the general form

$$\left\{k_1 J_m (\beta r) + k_2 N_m (\beta r)\right\} e^{-jm\phi}$$

where k_1 and k_2 are arbitrary constants. The index m is an integer and J_m and N_m are Bessel's functions of the 1st and 2nd kinds respectively.

For a resonator with N gaps, there are N/2 complete cycles in the electric field configuration around the anode. (See Figure 3.) This requires that m have the values

$$N/2,\ N,\ 3N/2,\ \ldots$$

The magnetic field in the interaction space can be expressed as

$$H_z = \sum_{n=-\infty}^{+\infty} \left\{k_{n1} J_{Nn/2} (\beta r) + k_{n2} N_{Nn/2} (\beta r)\right\} e^{j(\omega t - \frac{Nn\phi}{2})} \quad (4)$$

The constants k_{n1} and k_{n2} must be determined from the boundary conditions. Each term of this summation can be considered as a component rotating wave. The angular velocity of rotation is obtained from

$$\omega t - \frac{nN\phi}{2} = \text{constant}$$

or

$$\omega_n = \frac{d\phi}{dt} = \frac{2\omega}{nN} \quad (5)$$

Thus, the fastest of the component waves is the one for which $n = \pm 1$.

The corresponding electric fields are obtained by substituting equation (4) into (1) and (2). There results

$$E_r = \sum_{n=-\infty}^{+\infty} \frac{nN}{2\omega \in r} R_{Nn/2}(\beta r)\, e^{j(\omega t - \frac{nN\phi}{2})} \qquad (6)$$

$$E_\phi = \sum_{n=-\infty}^{+\infty} \frac{\beta}{j\omega \in r} R'_{Nn/2}(\beta r)\, e^{j(\omega t - \frac{nN\phi}{2})} \qquad (7)$$

In these equations, the function $-R_{Nn/2}(\beta r)$ has been substituted for $\left\{k_{n1} J_{nN/2}(\beta r) + k_{n2} N_{Nn/2}(\beta r)\right\}$.

Equations of Motion

Before discussing the rf fields any further, it will be instructive to consider the mechanism of exchange of energy between electrons and the rf field. A static radial field, and a constant axial magnetic field with both radial and angular components of rf electric field are assumed. The equations of motion of electrons in the interaction space then are

$$\frac{d}{dt}\left(m\frac{dr}{dt}\right) - mr\left(\frac{d\phi}{dt}\right)^2 = -eE_r - Ber\frac{d\phi}{dt}, \qquad (8)$$

and,

$$\frac{d}{dt}\left(mr^2\frac{d\phi}{dt}\right) = -erE_\phi + Ber\frac{dr}{dt}. \qquad (9)$$

Here B is in the positive z direction.

The 1st integral of equation (9) can be written as

$$mr^2 \frac{d\phi}{dt} = - e \int_{t_o}^{t} r E_\phi \, dt + Be \frac{r^2 - r_c^2}{2} \qquad (10)$$

where r_c is the cathode radius.

In the first term on the right-hand side, r is to be interpreted as the radius of a particular electron that starts out at the cathode at $t = t_o$, and E_ϕ is the angular component of the electric field at radius r. It is assumed that $\frac{d\phi}{dt} = 0$ at $r = r_c$ and $t = t_o$. If r(t) oscillates with frequency ω, this term can contribute a cumulative effect. This case is of little interest, however, as the magnetic field necessary to bring about this condition is relatively high. Another condition under which the integral can contribute a cumulative effect occurs if the angular position of the electron varies in such a way that E_ϕ is always positive (or negative). The expansion for E_ϕ (equation 7) shows that if the electron rotates with approximately the angular frequency of one of the rotating components, this component will cause the integral in equation (10) to build up cumulatively. The component with the same velocity as the electron is the part of E_ϕ which causes the effect to accumulate. All of the other components of E_ϕ then represent perturbations on the integral of frequency ω, 2ω, etc. Thus, the principal effect of the rf field on the electron velocities can be calculated from the single component of wave which is traveling with nearly the same velocity as the electrons.

It is possible to see how to produce an electron stream traveling with the same velocity as the rf wave by considering the behavior of a static magnetron, with voltage below the cut-off voltage. Appendix I considers the possible self-consistent space charge distributions in the presence of a purely static field for both planar and cylindrical geometries. Appendix I is concerned mainly with the V-I relationship and with electron trajectories when the magnetron is conducting current. If a voltage V_a, less than the cut-off voltage, is applied to the magnetron anode, electrons cannot reach the anode through static fields. If r_1 is taken as the maximum radius that the electrons can attain and V_1 the voltage at that radius, there must be a potential distribution inside the radius r_1 corresponding to a magnetron of anode radius r_1 at the cut-off voltage, but conducting zero net current. Outside the radius r_1, the space charge is zero, and there is a logarithmic potential distribution. At the edge of the electron cloud, the radial velocity is zero. It is shown in Appendix I that the potential and the angular velocity for the static magnetron are given by

$$V = \frac{1}{2} \frac{m}{e} \left\{ \left(\frac{dr}{dt} \right)^2 + \left(r \frac{d\phi}{dt} \right)^2 \right\} \qquad (10a)$$

and

$$r \frac{d\phi}{dt} = \frac{Be}{2m} r \left(1 - \frac{r_c^2}{r^2} \right) \quad . \qquad (10b)$$

From these one may obtain: $V = \frac{1}{2} \frac{m}{e} \left\{ \left(\frac{dr}{dt} \right)^2 + \left(\frac{Be}{2m} \right)^2 r^2 \left(1 - \frac{r_c^2}{r^2} \right)^2 \right\}$

and $$\frac{dV}{dr} = \frac{m}{e}\left\{\frac{d^2r}{dt^2} + \left(\frac{Be}{2m}\right)^2\left(r - \frac{r_c^2}{r}\right)\left(1 + \frac{r_c^2}{r^2}\right)\right\}. \quad (11)$$

It is seen that dV/dr is always finite. The radius r_1 is obtained by matching voltages and voltage gradients at the boundary r_1. For $r > r_1$ the potential is

$$V - V_1 = \frac{V_a - V_1}{\ln \frac{r_a}{r_1}} \ln \frac{r}{r_1} . \quad (12)$$

The voltage gradient for $r > r_1$ is

$$\frac{dV}{dr} = \frac{V_a - V_1}{\ln \frac{r_a}{r_1}} \frac{1}{r} . \quad (13)$$

Since the radial velocity is zero at the edge of the electron cloud,

$$V_1 = \frac{1}{2} \frac{m}{e} \left(\frac{Be}{2m}\right)^2 r_1^2 \left(1 - \frac{r_c^2}{r_1^2}\right)^2 \quad (14)$$

and, from matching the gradients at the boundary

$$V_a - V_1 = \frac{m}{e} \ln \frac{r_a}{r_1}\left\{r_1 \frac{d^2r}{dt^2} + \left(\frac{Be}{2m}\right)^2 r_1^2 \left(1 - \frac{r_c^2}{r_1^2}\right)\left(1 + \frac{r_c^2}{r_1^2}\right)\right\}. \quad (15)$$

It follows that

$$\frac{V_a}{V_c} = \frac{\left(r_1 - \frac{r_c^2}{r_1}\right)^2}{\left(r_a - \frac{r_c^2}{r_a}\right)^2} + 2 \ln \frac{r_a}{r_1}\left\{\frac{\frac{d^2r}{dt^2}}{r_a^2\left(1 - \frac{r_c^2}{r_a^2}\right)\left(\frac{Be}{2m}\right)^2} + \frac{(r_1^2 - r_c^2)\left(1 + \frac{r_c^2}{r_1^2}\right)}{\left(r_a - \frac{r_c^2}{r_a}\right)^2}\right\} \quad (16)$$

where V_c is the cut-off voltage (Eq. 107 Appendix I). In equation

(16), the radial acceleration $\frac{d^2r}{dt^2}$ is evaluated at the edge of the electron cloud.

If a space charge configuration is assumed in which the electrons move in circles around the cathode with zero radial velocity, this term is zero. If, however, there is a double stream of electrons as obtained in Appendix I for r_a/r_c very large, the radial acceleration is not zero at the edge of the space charge cloud. For r_a/r_c small, the acceleration at the edge of the space charge cloud becomes small, and in fact, is zero for a planar magnetron, and for the cylindrical magnetron with r_a/r_c up to about 2.5. Figures 4 and 5 show r_l/r_a plotted as a function of V_a/V_c for $r_a/r_c = 10$ and $r_a/r_c = 1.5$. For the plot of figure 4, curves are shown for the assumption of single stream and double stream where the accelerations are obtained from the calculations of Appendix I. In figure 5, it is assumed that the radial acceleration is zero at the edge of the cloud.

At the edge of the space charge region, the electrons travel with angular velocity as obtained from equation (10b)

$$\frac{d\phi}{dt} = \frac{Be}{2m}\left(1 - \frac{r_c^2}{r_l^2}\right) .$$

With proper adjustment of B and V_a, one can clearly obtain an electron stream which is traveling at the wave velocity. This interpretation certainly omits some very important features of the static magnetron. In particular, there is conduction of current

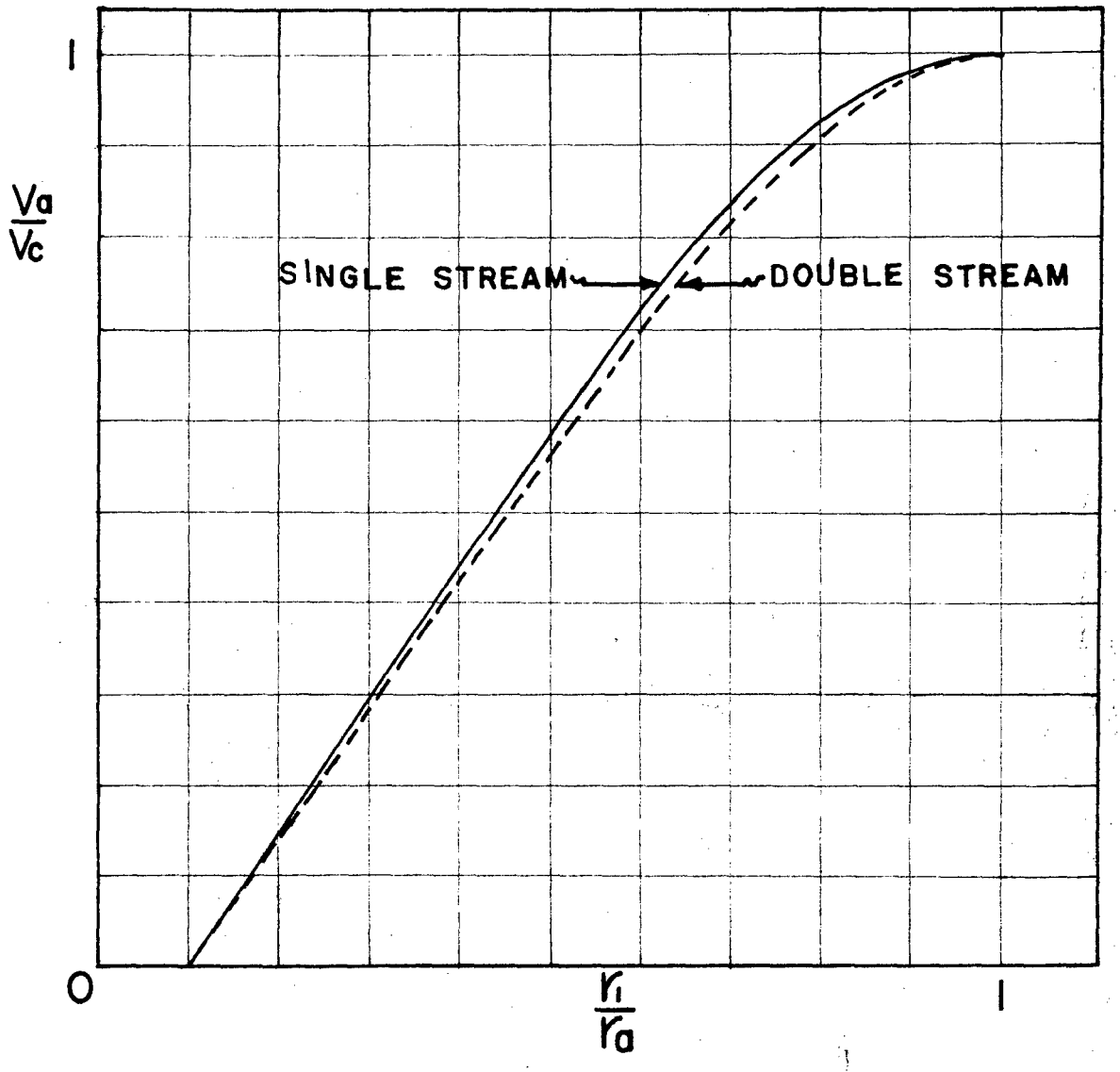

Figure 4

Relative radius of electron cloud r_1/r_a as a function of relative anode voltage V_a/V_c for $r_a/r_c = 10$.

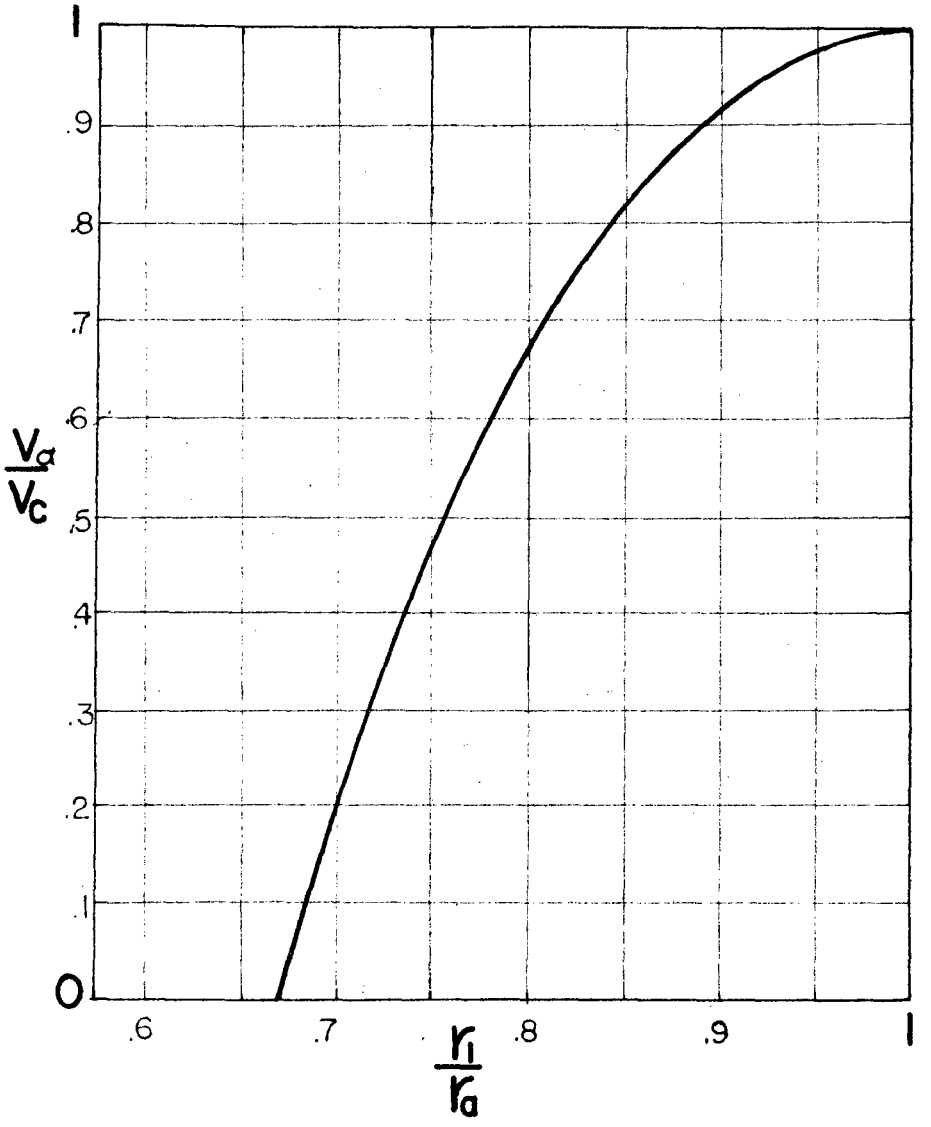

Figure 5

Relative radius of electron cloud r_1/r_a as a function of relative anode voltage V_a/V_c for $r_a/r_c = 3/2$.

below the cut-off voltage and back bombardment of the cathode. (4) These phenomena are closely related. The violation of the cut-off condition and back bombardment of the cathode become more pronounced at high voltages, and must be a considerable factor in the behavior of magnetrons at high voltages. The effect is undoubtedly present at low voltages, but a theory which neglects these effects should give a zero-order approximation to the actual behavior. This approximation is illustrated by the relative success of the simplified theory in predicting the operating voltages and fields and the electronic efficiency of the ordinary traveling-wave type magnetron.

A physical explanation of the mechanism by which the ordinary magnetron oscillates is the following. Just before oscillation there is a sheath of electrons surrounding the cathode. The outermost of these electrons are traveling with approximately the same velocity as the rf wave when it is present. Small rf voltages build up, and the electrons lose energy to the traveling wave and move out toward the anode due to the fact that their angular velocity is lessened. The factor $d\phi/dt$ is very nearly constant in equations (8), (9) and (10), after the electron departs from the electron sheath around the cathode.

An electron, which is to travel ultimately from cathode to anode, leaves the cathode and is accelerated through the space charge sheath around the cathode. As it approaches the outside of

the space charge sheath, it experiences a retarding force due to the rf field which is present. This rf field forces the electron to maintain a relatively constant angular velocity. The dc field pulls the electron out toward the anode. During most of the trajectory the electron is controlled by the rf field. Near the cathode the electron is accelerated outward and acquires angular momentum in essentially a dc phenomenon until its angular velocity becomes ω_1, the angular velocity of the rotating wave. At this time the angular velocity becomes essentially constant.

Denote as r_1 the radius at which the angular velocity $d\phi/dt$ becomes ω_1 and call the voltage at this radius V_1. The angular velocity ω_1 is, from equation 106 (Appendix I)

$$\omega_1 = \frac{Be}{2m}\left(1 - \frac{r_c^2}{r_1^2}\right) \quad . \tag{17}$$

Radial velocities will be neglected so that

$$e V_1 = \frac{1}{2} m \omega_1^2 r_1^2 \tag{18}$$

the total kinetic energy of the electron, which is rotational.

For the space outside $r = r_1$, the assumption that $d\phi/dt = \omega_1$ and $dr/dt = 0$ in equation (8) results in

$$e (dV/dr) = (Be \omega_1 - m\omega_1^2) r \quad . \tag{19}$$

Integration of (19) yields

$$e (V - V_1) = (Be \omega_1 - m\omega_1^2) \frac{(r^2 - r_1^2)}{2} \quad . \tag{20}$$

Equation (20) will be reduced to dimensionless variables using

$$V/V_0 \quad \text{and} \quad B/B_0$$

where V_0 and B_0 are defined respectively by

$$e V_0 = \frac{1}{2} m r_a^2 \omega_1^2 \tag{21}$$

and

$$\omega_1 = \frac{B_0 e}{2m} \left(1 - \frac{r_c^2}{r_a^2}\right) . \tag{22}$$

Thus it is seen that V_0 is the voltage necessary to give the electron the velocity $r_a \omega_1$ and B_0 is the magnetic field which will give the electron angular velocity ω_1 at the anode if it travels from cathode to anode in static fields. In terms of these variables, the Hull cut-off voltage, as given by equation (107), Appendix I, may be expressed as

$$V/V_0 = (B/B_0)^2 \tag{23}$$

This equation is obtained by dividing equation (107) by equation (21) and then eliminating ω_1 by using equation (22).

In equation (20), V_1 and r_1 are functions of B in general. The particular functions are given in (17) and (18), which may be used to eliminate V_1 and r_1 in (20). Then, with $r = r_a$, there results

$$V/V_0 = \frac{2B}{B_0} - 1 \quad . \tag{24}$$

This is the Hartree relation and represents the minimum voltage that allows electrons to flow to the anode in the presence of an rf field.[5] The graph (Fig. 6) shows the cut-off curve and Hartree curve, in terms of dimensionless variables. The Hartree curve is tangent to the cut-off curve at $V = V_0$, $B = B_0$.

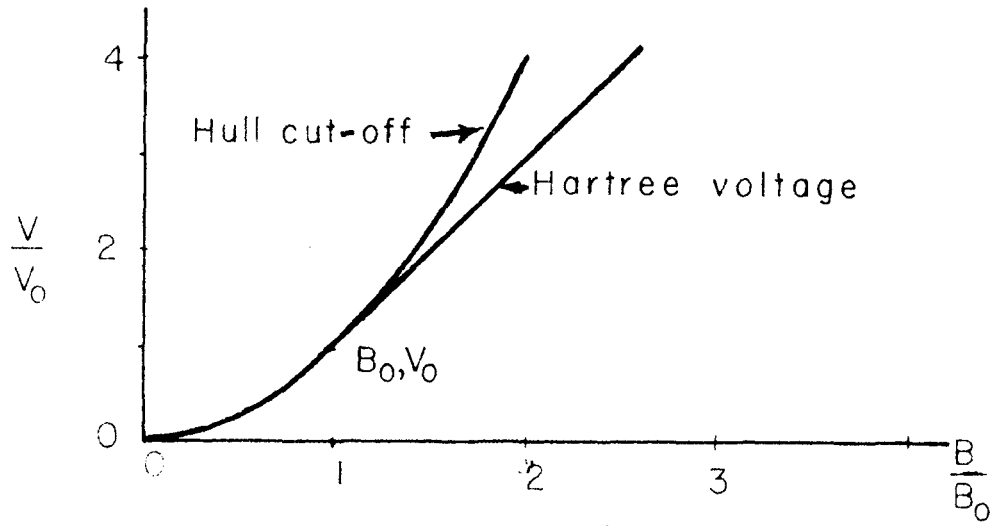

Figure 6

Normalized Cut-off curve and Hartree curve.

Normal traveling-wave magnetrons operate near the Hartree curve at values of B several times B_0. It is the purpose of this discussion to consider the optimum type of operation at values of B near $B = B_0$. It is illuminating to consider the dependence of r_1 (see equation 17) on B/B_0 near $B = B_0$. Substituting for ω_1 in terms of B_0 (equation 22), one obtains

$$\frac{r_c^2}{r_1^2} = 1 - \frac{B_0}{B}\left(1 - \frac{r_c^2}{r_a^2}\right) . \qquad (25)$$

The implications of this equation are considered in the following discussion. Figure 7 shows the dependence implied in equation (25) for various values of r_c/r_a. For each cathode size, $r_l = r_a$ at $B = B_0$. To satisfy the requirements of the physical picture of the electron-field interaction, the electrons must become synchronous with the traveling wave at a radius where the rf field is strong enough to change the electronic velocity. On the other hand, the radius where synchronism occurs must not be so great that there is no space in which the electrons can deliver energy to the rf field. Since the synchronous radius is a function of both r_c/r_a and B/B_0, the correct cathode size is dependent on the range of B/B_0 in which it is desired to operate. If one considers the extreme case of $r_c/r_a = 0.1$ and $B/B_0 = 1.3$, the radius at which the electrons are synchronous with the traveling wave is $0.2\, r_a$. At this radius the rf field strength for an 18 vane anode operating in the π-mode is approximately 2×10^{-6} of the field strength at the anode, as determined by equation (27).

Thus even for relatively large rf fields at the anode, the field strength at the radius where the electrons and the electric field are synchronous is extremely small. If the rf field intensity is less than that resulting from the noise fluctuations of the electrons themselves, the electrons could not be expected to deliver energy

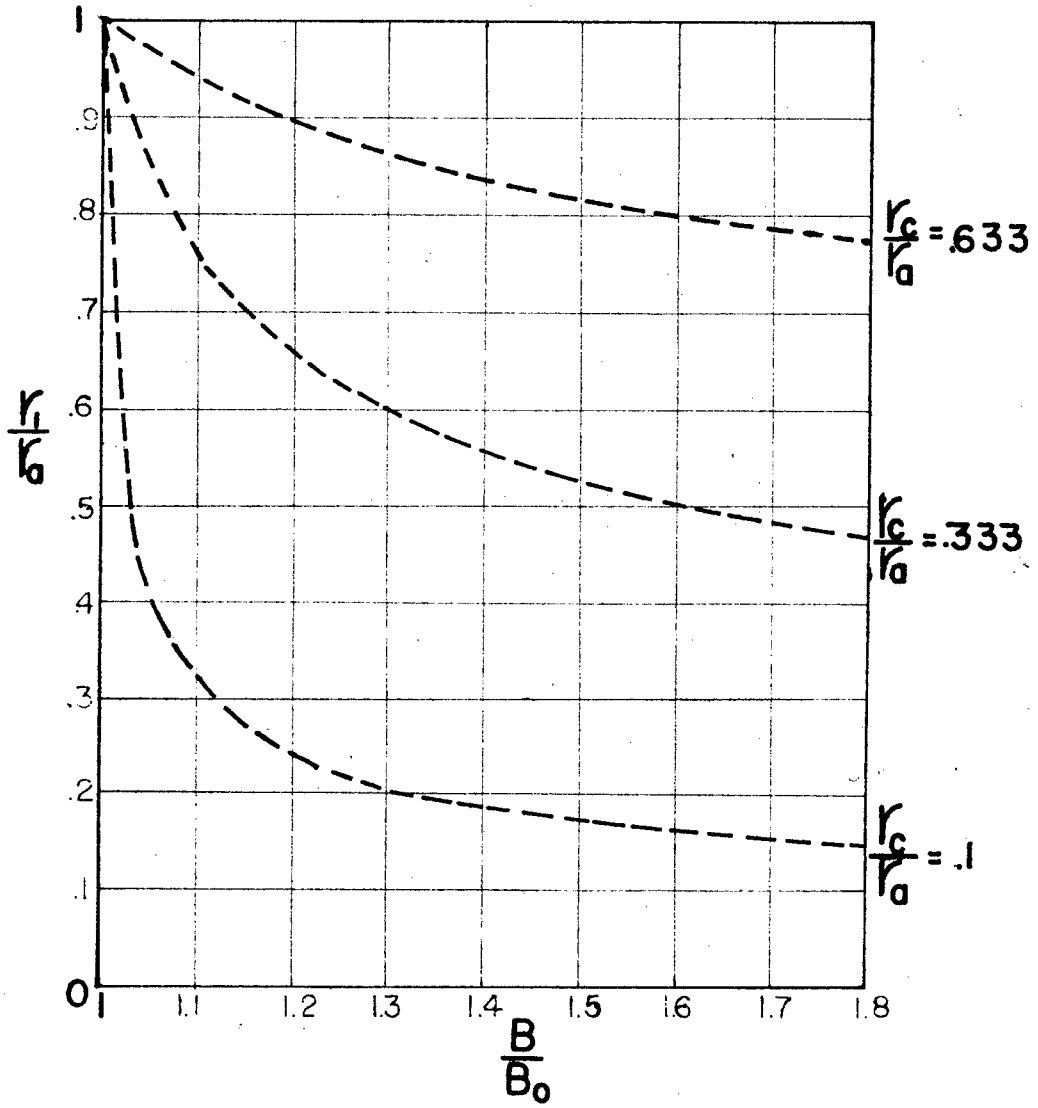

Figure 7

Synchronous radius r_1 as a function of

B/B_0 and r_c/r_a.

to the ac field. If the cathode is too small, the rotating electron space charge cloud is not coupled sufficiently closely to the rf field to allow the magnetron to oscillate in the normal manner.

Conversely, if the cathode is too large, the electrons do not become synchronous with the rf field until they are almost at the anode, thus not making use of the rf field. Also, the cathode partially shorts out these fields. This results in a reduction in efficiency of operation.

In order to give approximately correct coupling, the synchronous radius should occur at approximately the radius where the amplitude of the rf field is a given fraction of the amplitude at the anode. This means that the ratio r_c/r_a is a function of B/B_0, the ratio of magnetic field to characteristic magnetic field, as well as N, the number of vanes. Figure 8 shows the value of r_c/r_a for various values of synchronous radii as a function of B/B_0. In every case, the cathode radius approaches zero as B/B_0 approaches unity. From this one might conclude that to operate a magnetron very near the characteristic magnetic field, one must have a cathode of very small radius.

Cathode Size for Normal Type Magnetrons

The concept of energy exchange supplies a clue as to the correct cathode size for operation at values of B several times B_0. Since the curves of figures 7 and 8 flatten out as B becomes several

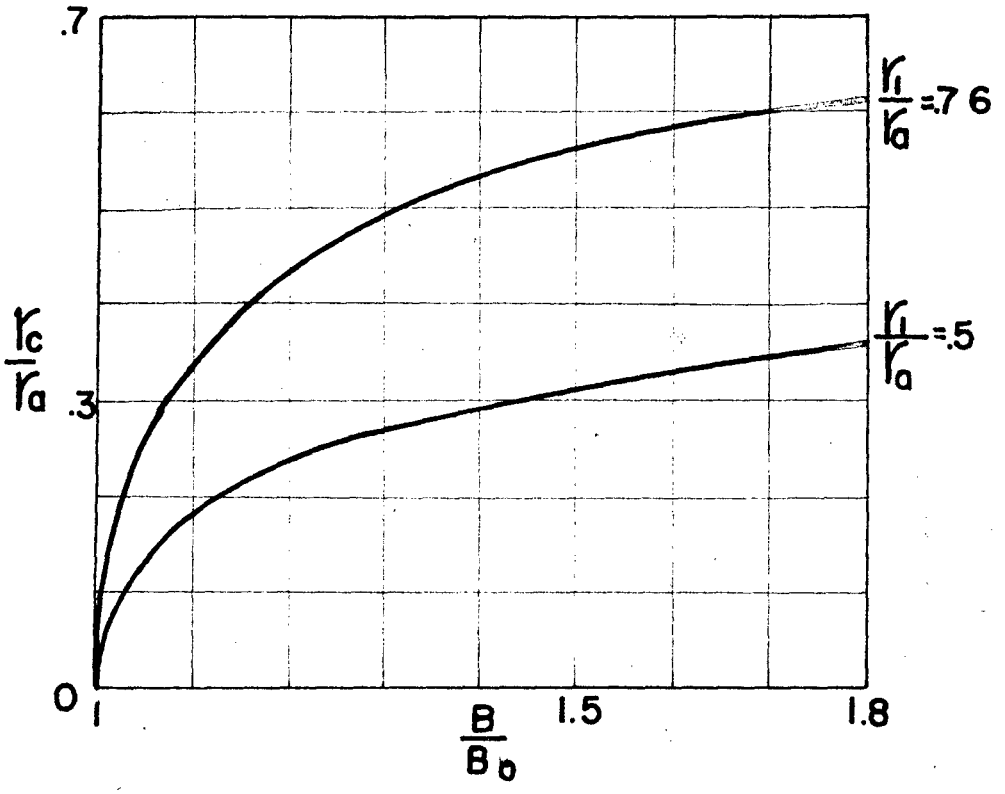

Figure 8

Cathode size as a function of B/B_0 for various synchronous radii.

times B_0, the cathode radius should be relatively independent of B/B_0 for a large range of B. Assuming that the resonator is to operate in the π-mode, if the cathode is too small, or too far away from the anode, the oscillator will have a tendency to operate in the wrong mode because the electric field associated with the proper mode may be too weak at the edge of the space charge sheath. This may allow the magnetron to start oscillating in a mode different from the proper one. On the other hand, if the cathode is too large or too near the anode, oscillations will be inefficient because part of the rf fields are shorted out. A formula that places the cathode at approximately the correct distance from the anode for normal operation is

$$\frac{r_c}{r_a} = \frac{N - 4}{N + 4} \tag{26}$$

The tangential electric field at the cathode is, of course, zero; but if the field E_ϕ is calculated in the absence of the cathode, the cathode surface comes at the radius where this field component has fallen to about 3% of its value at the anode. Referring to equation (7), if there is no cathode, the function $R_{Nn/2}(\beta r)$ must be replaced by $J_{Nn/2}(\beta r)$, the Bessel's function of the first kind. Since r_a is a small part of a wavelength, $J_{Nn/2}(\beta r)$ can be replaced approximately by $\frac{(\beta r/2)^{Nn/2}}{Nn/2\ !}$. Considering only the

fundamental space component of the wave, one has

$$\frac{E_\phi}{E_{\phi_a}} = \frac{r}{r_a}^{N/2 - 1} \tag{27}$$

where E_{ϕ_a} is the amplitude of the fundamental component of the traveling wave at the anode, and E_ϕ is the amplitude of the same wave at radius r. If E_ϕ/E_{ϕ_a} is taken as 1/30 and $r = r_c$, one obtains the design formula

$$\frac{r_c}{r_a} = \frac{1}{30^{\frac{1}{N/2 - 1}}}. \tag{28}$$

This is compared with $(N - 4)/(N+4)$ for a range of N from 4 to 38, and with actual values used in normal traveling wave type magnetrons in the following table:

N	$\frac{1}{30^{\frac{1}{N/2 - 1}}}$	$\frac{N - 4}{N + 4}$	Value Used in Actual Tubes
4	.033	0.	.152
8	.322	.33	.35
10	.427	.428	.500
12	.506	.50	.5 - .58
16	.615	.600	.59 - .66
18	.655	.637	.6 - .62
20	.685	.667	.6 - .61
26	.755	.733	.707
38	.828	.81	.76

It is evident from the tabulation that the actual departure of commercial magnetrons from the condition that $\frac{r_c}{r_a} = \frac{N - 4}{N + 4}$ is

about as great as from the condition imposed by equation (28).

Transition to Low Field

The picture of the mechanism of oscillation in the magnetron must be altered somewhat to account for the phenomena at low fields. It is well known that an electron stream traveling with very nearly the same velocity as an rf wave will exchange energy with the wave. (This is the operating principle of the traveling wave tube.) Suppose, for example, that a very small cathode (say $r_c/r_a = 0.1$) is used in an 18 vane magnetron with B/B_0 set at 1.2. The radius at which the electron stream becomes synchronous is approximately $0.25\ r_a$. For π-mode operation of an 18 vane magnetron, the rf field would not appreciably affect the trajectories at this radius. As the anode voltage is raised closer to cut-off the electron trajectories will come nearer the anode and into a region of greater rf field intensity. The angular velocity of the electrons at a given radius is proportional to B, the magnetic field, if the electron traveled to the radius through static fields. Hence the velocity of the electrons will not exceed that of the rotating wave by a fraction greater than $(B/B_0 - 1)$ so that there is still the possibility of energy exchange and oscillation for B/B_0 in the vicinity of 1. If a small cathode is used, the angular velocity as given by equation 106 is almost constant throughout the trajectory. However, as B/B_0 is made much larger than 1, the velocity of the

electrons begins to differ too greatly from that of the wave, and there is no exchange of energy. Thus for small cathodes, there should be a maximum magnetic field at which the magnetron will work. Also for small cathodes, the voltage at which the magnetron starts to oscillate should be determined by the anode voltage necessary to pull the electrons out to the region of strong rf fields.

In experimental magnetrons built at The Ohio State University Electron Tube Laboratory, qualitative agreement with these conclusions has been obtained. These experiments are described in detail in a later section. The following section consists of a theoretical verification of the proposed concept of energy exchange for magnetrons operating at low fields.

The Electron-Electric Field Interaction

A more detailed theory of operation requires the actual calculation of electron trajectories in order to obtain the electronic energy at the anode and, hence, the electronic efficiency. In experimental models built in the Electron Tube Laboratory, it has been observed that the voltage-current relation is essentially the same whether the magnetron is oscillating or not. From this fact we can conclude that even in the absence of an rf field the trajectories pass close to the anode. Figure 9 shows the cut-off curve, Hartree curve and the voltages which are necessary to pull the electrons out to 0.8 and 0.9 of the anode radius, assuming $r_c/r_a = 0.1$. The last two

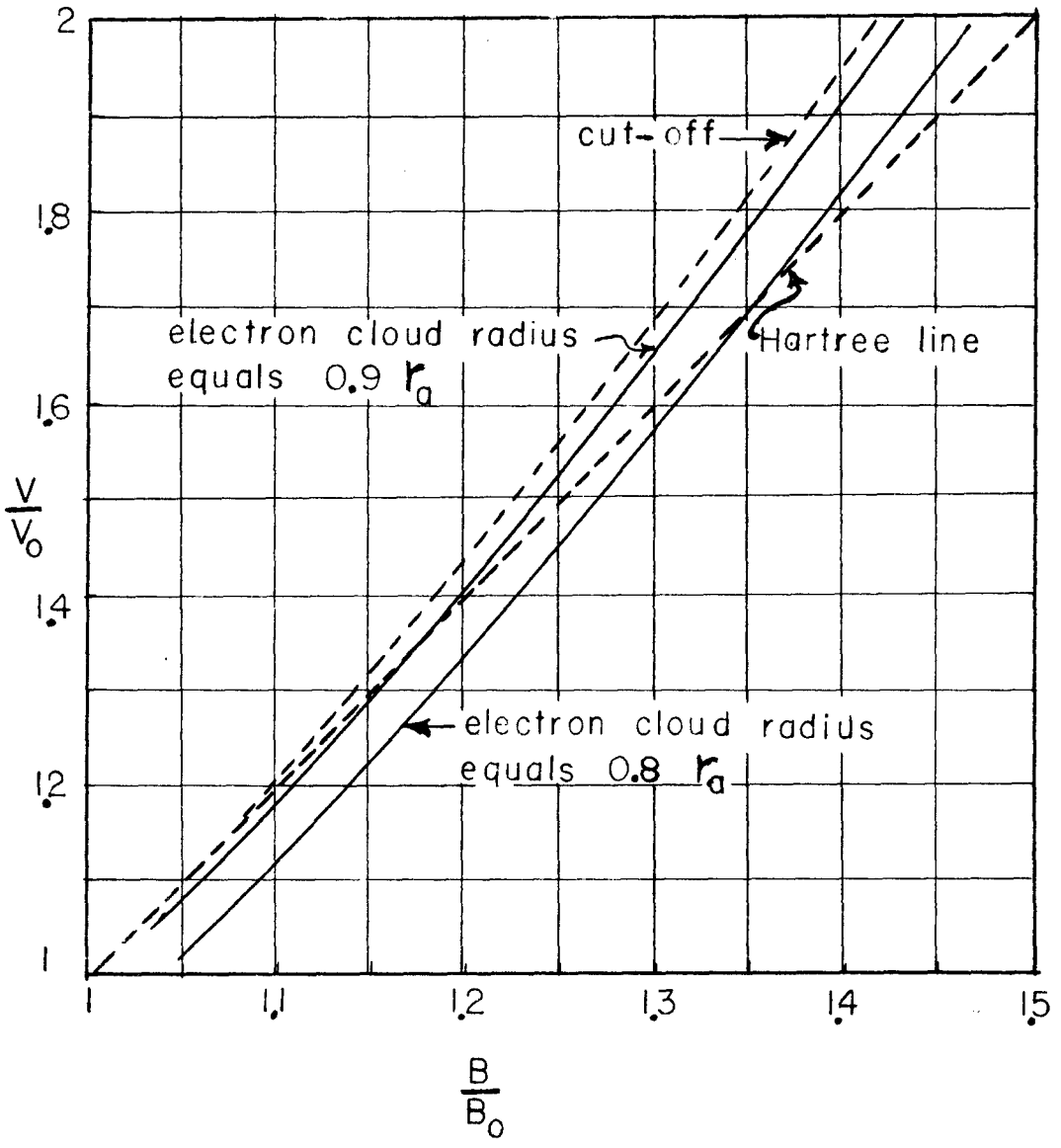

Figure 9.

Voltages necessary to produce electron cloud radii of $0.8\ r_a$ and $0.9\ r_a$, $r_a/r_c = 10$.

curves are obtained from Fig. 4 and are approximately 93% and 98% of the cut-off voltage. A reduction of 7% in voltage under oscillatory conditions could certainly be detected experimentally; but a reduction of 2% could not be detected with the accuracy of available instruments. In fact, the wave guide tuner does have a very slight effect on the magnetron current and voltage. If the tuner is adjusted to give vigorous oscillations, the anode voltage at a given current is 1% approximately less than if there are no oscillations.

In Appendix I the potential distribution is obtained for a 2-stream condition in a magnetron at cut-off. Figure 10 and Fig. 11 show the distribution assuming that the edge of the static electron cloud is 0.8 and 0.9 of the anode radius. Because of the space charge effects, the potential is almost linear inside the space charge cloud for the 2-stream case. In fact, if the voltage gradient is assumed constant and trajectories are calculated, they agree very well with those calculated from the exact equations.

The potential distribution for the self-consistent solution below cut-off in which the electrons all have zero radial velocity is also plotted. In Appendix I, it is shown that there is no single stream solution in which a net current less than about 3/4 of the Langmuir current (less than the Allis Current) can be conducted. The only possible space charge condition for small cathode diameters is the 2-stream solution in which the arithmetical sum of the currents is

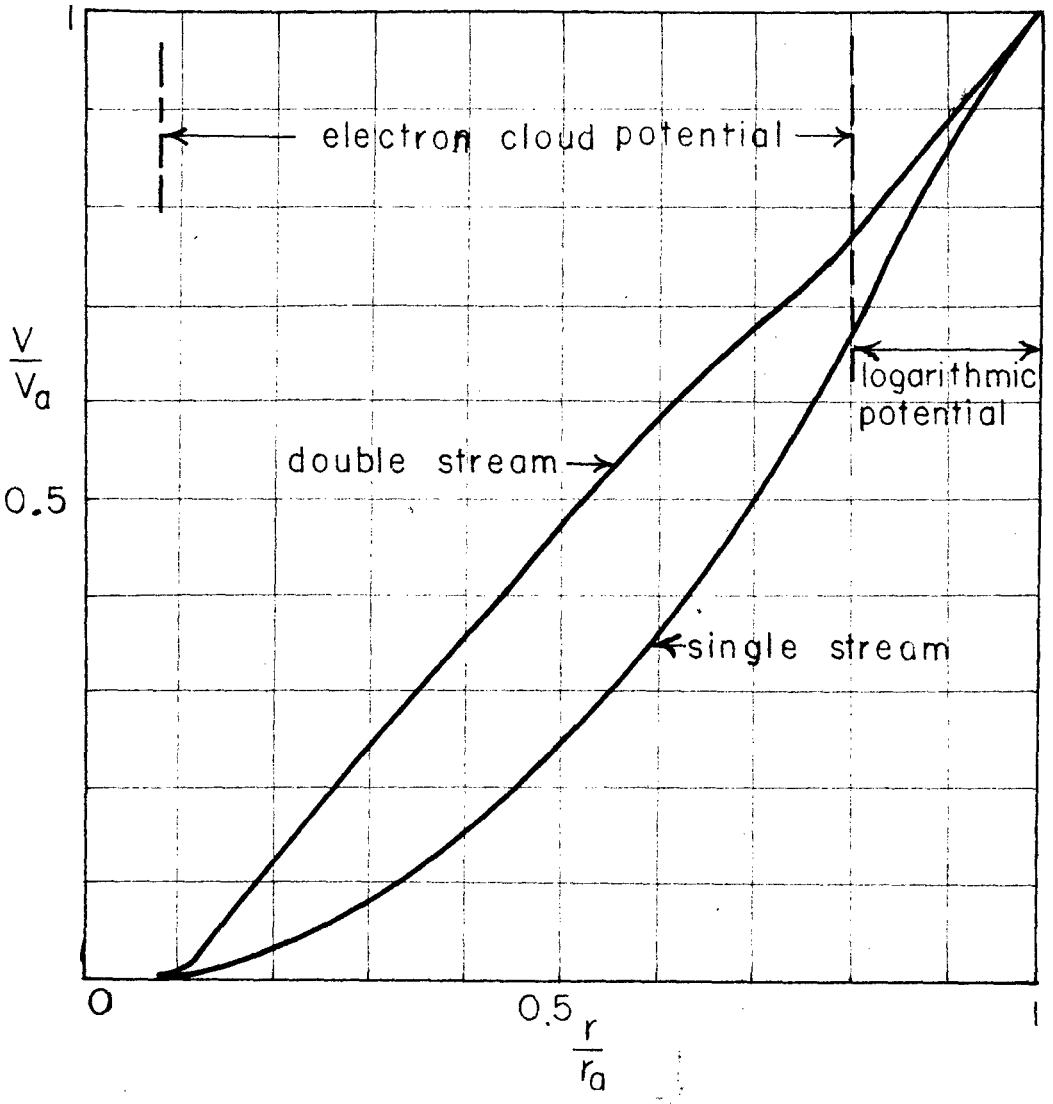

Figure 10

Potential distribution in static magnetron with radius of electron cloud = 0.8 r_a, $r_a/r_c = 10$.

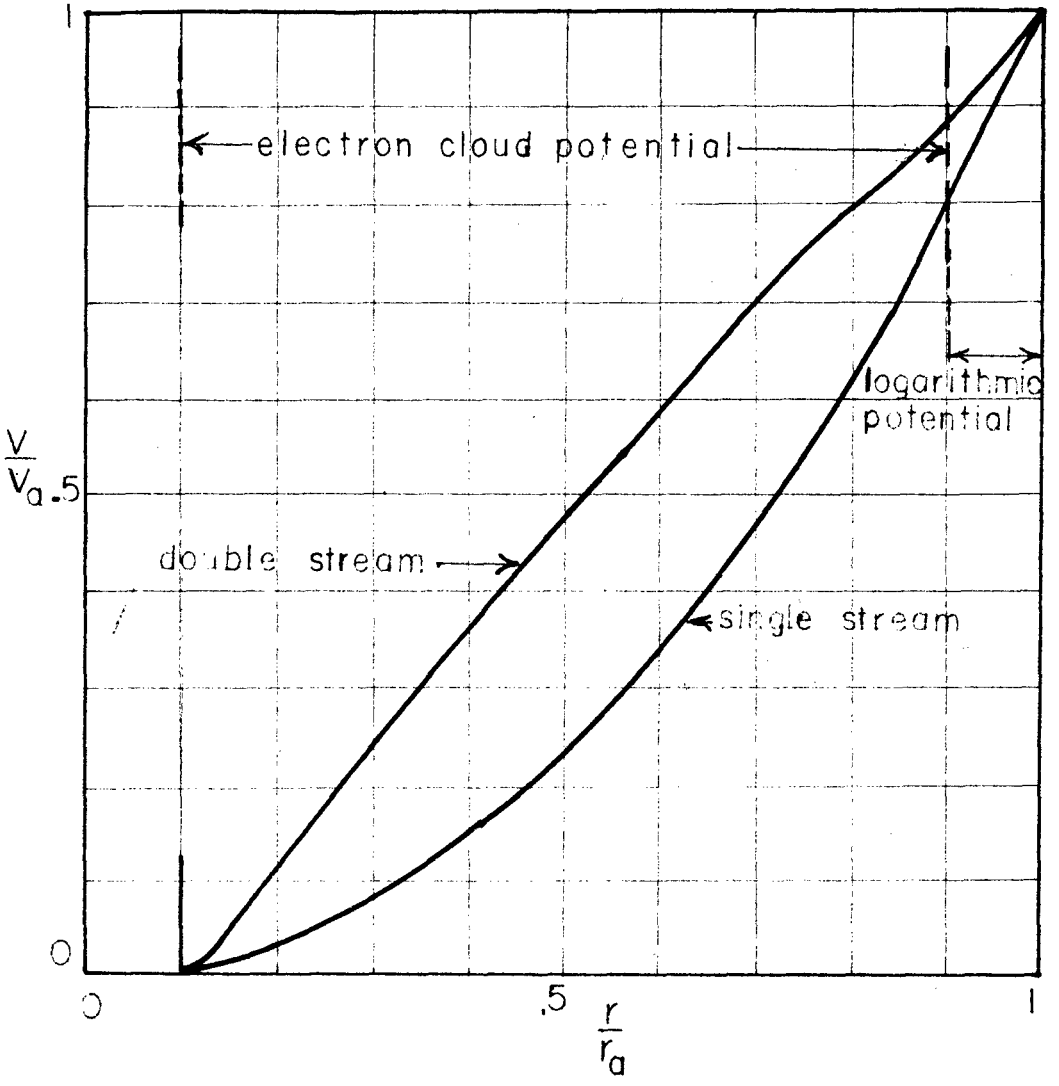

Figure 11

Potential distribution in static magnetron with radius of electron cloud $0.9\ r_a$, $r_a/r_c = 10$.

the Allis current while the algebraic sum is the net current. This matter is discussed more completely in Appendix I.

If a constant dc potential gradient is assumed, the differential equations of motion are

$$\frac{d^2 r}{dt^2} - r \left(\frac{d\phi}{dt}\right)^2 = \frac{e}{m} \frac{V_a}{r_a - r_c} - \frac{e}{m} E_{rac} - \frac{Ber}{m} \phi \quad (29)$$

$$\frac{d}{dt}\left(r^2 \frac{d\phi}{dt}\right) = - \frac{e}{m} r E_\phi + \frac{Be}{m} r \frac{dr}{dt} , \quad (30)$$

where the radial field is assumed to be

$$E_r = - \frac{V_a}{r_a - r_c} + E_{rac} . \quad (31)$$

These equations should give a fairly good approximation to the dynamic behavior of the magnetron if the space charge cloud very nearly fills the interaction space.

The specific form for the rf fields must be obtained in order to proceed with the dynamic solution of the problem. Since the low field magnetron works best with a small cathode, approximations consistent with the use of small cathode radii will be used. Furthermore, it is true of all practical magnetrons that the anode radius is a small part of a wavelength -- so that $\beta r_a/2$ is no greater than 1/2.

The expression for the space fundamental component of the traveling waves in the interaction region is obtained from equation (4).

$$H_{z1} = \left\{ k_{11} J_{N/2} (\beta r) + k_{12} N_{N/2} (\beta r) \right\} e^{j(\omega t - N\phi/2)} \qquad (32)$$

Substitution of this expression into equation (2) gives the corresponding component of E_ϕ.

$$E_{\phi 1} = - \frac{\beta}{j \omega \epsilon} \left\{ k_{11} J'_{N/2} (\beta r) + k_{12} N'_{N/2} (\beta r) \right\} e^{j(\omega t - N\phi/2)} \qquad (33)$$

It is necessary that E_ϕ be zero at $r = r_c$. Hence,

$$k_{11} J'_{N/2} (\beta r_c) + k_{12} N'_{N/2} (\beta r_c) = 0 \qquad (34)$$

or

$$k_{12} = - k_{11} \frac{J'_{N/2} (\beta r_c)}{N'_{N/2} (\beta r_c)} \qquad (35)$$

Thus,

$$E_{\phi 1} = - \frac{\beta k_{11}}{j \omega \epsilon} \left\{ J'_{N/2} (\beta r) - \frac{J'_{N/2} (\beta r_c)}{N'_{N/2} (\beta r_c)} N'_{N/2} (\beta r) \right\} e^{j(\omega t - N\phi/2)} \qquad (36)$$

The use of an approximation for Bessel's functions for small values of the argument yields

$$N_{N/2}(\beta r) = - \frac{(N/2 - 1)! 2^{N/2}}{\pi (\beta r)^{N/2}} \left\{ 1 + \frac{(\beta r/2)^2}{N/2 - 1} + \frac{(\beta r/2)^4}{2(N/2 - 1)(N/2 - 2)} + \ldots \right\} \qquad (37)$$

$$J_{N/2} (\beta r) = \frac{1}{(N/2)!} (\beta r/2)^{N/2} \left\{ 1 - \frac{(\beta r/2)^2}{N/2 + 1} + \ldots \right\} \qquad (38)$$

If $(\beta r/2)$ is not greater than 1/2 and N = 18, the first term of the expansions gives a good approximation to the functions. Thus,

$$N'_{N/2}(\beta r) = \frac{(N/2 - 1)!\,(N/2)\,2^{N/2}}{(\beta r)^{N/2+1}} \tag{39}$$

$$J'_{N/2}(\beta r) = \frac{1}{2\,(N/2 - 1)!}\,(\beta r/2)^{N/2 - 1} \tag{40}$$

Substitution of these approximate expressions into equation (32) gives the result

$$k_{12} = -k_{11}\,\frac{\pi\,(\beta r_c/2)^N}{N/2\,!\,(N/2 - 1)!} \tag{41}$$

Thus equation (36) becomes

$$E_{\phi 1} = \frac{-\beta k_{11}}{j\omega \in}\left\{J'_{N/2}(\beta r) - \frac{\pi\,(\beta r_c/2)^N}{N/2\,!\,(N/2 - 1)!}\,N'_{N/2}(\beta r)\right\}e^{j(\omega t - N\phi/2)}$$

Consideration of a practical case will give an idea of the order of magnitude of the two terms. Thus, let it be assumed that $(\beta r_a/2) = 0.5$ and $(\beta r_c/2) = 0.05$ and $N = 18$. Then,

$$\frac{\pi\,(\beta r_c/2)^{18}}{9!\;8!} \cong .85 \times 10^{-33} \tag{42}$$

At $(\beta r/2) = 0.05$, the two terms are equal and cancel out. The first term increases as r^8, and the second term decreases as r^{-10}. At $(\beta r/2) = 0.1$ the ratio of the 1st term to the 2nd one is 2^{18}. Thus the part of the field contributed by the Bessel's function of the 2nd kind is insignificant compared to the Bessel's function of the 1st kind. If only the Bessel's function of the 1st kind and the 1st term in the expansion of this function are kept,

equation (32) becomes

$$H_{z1} = C\,(\beta r/2)^{N/2}\, e^{j(\omega t - N\phi/2)} \tag{43}$$

In this equation, C is a constant to be determined by conditions at the anode. For the evaluation of C, it will be assumed that the average rf voltage along the ϕ-coordinate line at $r = r_a$ is the same as the average of the fundamental rotating components. For this purpose, it is necessary to obtain the standing wave resulting from oppositely rotating components. Thus,

$$H_{z1}^{*} = 2C\,(\beta r/2)^{N/2}\,(\cos N\phi/2)\, e^{j\omega t} \tag{44}$$

$$E_{r1}^{*} = -\frac{NC}{j\omega \epsilon r}\,(\beta r/2)^{N/2}\,\sin(N\phi/2) e^{j\omega t} \tag{45}$$

$$E_{\phi 1}^{*} = -\frac{NC}{2j\omega \epsilon}\,(\beta r/2)^{N/2 - 1}\,\cos(N\phi/2)\, e^{j\omega t} \tag{46}$$

The * will be used to designate the sum of oppositely traveling wave components. It has been tacitly assumed that E_ϕ is symmetric about the coordinate $\phi = 0$. This will happen if a gap in the anode is centered around $\phi = 0$, as in Figure 12.

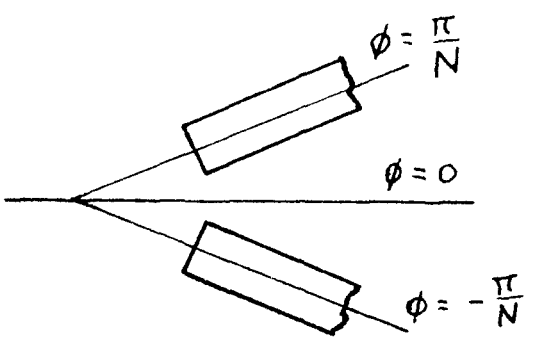

Figure 12
Orientation of magnetron anode.

A voltage $V_1 e^{j\omega t}$ will be assumed across this gap. The constant C is determined from the condition

$$V_1 e^{j\omega t} = \int_{-\pi/N}^{\pi/N} E^*_{\phi 1} r_a \, d\phi \tag{47}$$

where $E^*_{\phi 1}$ is evaluated at $r = r_a$ or

$$C = - \frac{j \omega \in}{4 (\beta r_{a/2})^{N/2}} V_1 \tag{48}$$

Substitution for C in equations (42) and (43) gives

$$E^*_{r1} = (NV_{1/4r}) (r/r_a)^{N/2} \sin (N\phi/2) e^{j\omega t} \tag{49}$$

$$E^*_{\phi 1} = (NV_1/4r) (r/r_a)^{N/2} \cos (N\phi/2) e^{j\omega t} \tag{50}$$

The equations of motion and the formulae for E_r and E_ϕ will be expressed in terms of dimensionless variables

$$R = r/r_a \tag{51}$$

$$\tau = \frac{(B e) t}{2m} = \omega_L t \tag{52}$$

Alternate forms of E_{r1} and $E_{\phi 1}$ including time variation are

$$\mathrm{Re}\left[E^*_{r1}\right] = \frac{NV_1}{4 r_a} R^{(N/2 - 1)} \sin (N\phi/2) \cos (\omega/\omega_L \tau + \alpha) \tag{53}$$

$$\mathrm{Re}\left[E^*_{\phi 1}\right] = \frac{NV_1}{4 r_a} R^{(N/2 - 1)} \cos (N\phi/2) \cos (\omega/\omega_L \tau + \alpha) \tag{54}$$

In these equations, an initial phase angle α is introduced to allow for electrons starting their trajectories at various parts of the cycle. Real parts have been taken.

Another representation of the field is in terms of rotating components. The rotating components of the wave are obtained by expressing the products of the trigonometric functions in equations (53) and (54) as the sum of the two functions using trigonometric identities. The two resulting terms represent oppositely rotating waves. The components which rotate in the $+\phi$ direction are

$$E_{r1} = - \frac{NV_1}{8 r_a} R^{(N/2 - 1)} \sin (\omega/\omega_L \tau - N\phi/2 + \alpha) \tag{55}$$

$$E_{\phi 1} = \frac{NV_1}{8 r_a} R^{(N/2 - 1)} \cos (\omega/\omega_L \tau - N\phi/2 + \alpha) \tag{56}$$

If an electron stream is traveling in the $+\phi$ direction with velocity very nearly the same as the rotating component of wave, the component which rotates in the opposite direction will result in perturbations of frequency 2ω. Thus it is not possible for the interaction of the electrons with the wave which travels in the negative direction to be cumulative. For this reason, only the component which travels in the $+\phi$ direction will be retained.

Substitution of dimensionless variables in the equations of motion (29) and (30) yields

$$\frac{d^2 R}{d\tau^2} = R (d\phi/d\tau)^2 + 2R (d\phi/d\tau) + \frac{e V_a}{m \omega_L^2 r_a (r_a - r_c)} - \frac{e E_{rac}}{m \omega_L^2 r_a} \tag{57}$$

$$\frac{d}{d\tau}\left(R^2 \frac{d\phi}{d\tau}\right) = 2R \frac{dR}{d\tau} - \frac{e}{m \omega_L^2 r_a} R E_{\phi ac} \qquad (58)$$

Replacing E_{rac} and $E_{\phi ac}$ by the expression (55) and (56) gives the result

$$\frac{d^2R}{d\tau^2} = R\left(\frac{d\phi}{dt}\right)^2 + 2R \frac{d\phi}{dt} + \frac{e V_a}{m \omega_L^2 r_a (r_a - r_c)}$$

$$+ \frac{e N V_1}{8 m \omega_L^2 r_a^2} R^{(N/2 - 1)} \sin (\omega/\omega_L \tau - N\phi/2 + \alpha) \qquad (59)$$

$$\frac{d}{d\tau}\left(R^2 \frac{d\phi}{d\tau}\right) = 2R \frac{dR}{d\tau} - \frac{e N V_1}{8m \omega_L^2 r_a^2} R^{N/2} \cos (\omega/\omega_L \tau - N\phi/2 + \alpha) \qquad (60)$$

These equations can be further simplified by using the cut-off relation (equation 107) which can be expressed as

$$e V_c = \frac{1}{2} m \omega_L^2 r_a^2 \left(1 - \frac{r_c^2}{r_a^2}\right)^2 \qquad (61)$$

The equations of motion become

$$\frac{d^2R}{d\tau^2} = R\left(\frac{d\phi}{dt}\right)^2 + \frac{V_a}{2V_c}\left(1 + \frac{r_c}{r_a}\right)\left(1 - \frac{r_c^2}{r_a^2}\right) + 2R \frac{d\phi}{dt}$$

$$+ \frac{N V_1}{16 V_c}\left(1 - \frac{r_c^2}{r_a^2}\right)^2 R^{(N/2 - 1)} \sin\left(\frac{\omega}{\omega_L} \tau - \frac{N\phi}{2} + \alpha\right) \qquad (62)$$

$$\frac{d}{dt}\left(R^2 \frac{d\phi}{dt}\right) = 2R \frac{dR}{dt} - \frac{N V_1}{16 V_c}\left(1 - \frac{r_c^2}{r_a^2}\right)^2 R^{(N/2 - 1)} \cos\left(\frac{\omega}{\omega_L} \tau - \frac{N\phi}{2} + \alpha\right) \qquad (63)$$

For any reasonable value of N, it is impossible to solve these equations analytically. A possible approach is to use a perturbation theory, either in stationary or rotating coordinates. This does not seem to be a fruitful course of action. Solutions were obtained for equations (62) and (63) for a range of values of α and $NV_1/\ 16V_c(1 - r_c^2/r_a^2)^2$ for N = 18 and $r_c/r_a = 0.1$ using the REAC analogue computer at Wright Field. A value of 1/2 was taken for $(V_a/2V_c)(1 + r_c/r_a)(1 - r_c^2/r_a^2)$. This means that $V_a = 0.91V_c$. Under static conditions, the edge of the electron cloud is at R = .88 or .90 depending on the space charge configuration, as obtained from Figure 4. This value is obtained from "exact" calculation of potentials. The value obtained by the computer using the approximate voltage distribution was 0.875. An elementary calculation of the static voltage at R = 0.875 and of the cut-off voltage at this same radius show the two to be the same, as expected.

The electronic efficiency is

$$\eta_e = 1 - \frac{1}{2} m \frac{\bar{v}^2}{eV_a} . \qquad (64)$$

In this equation $\bar{v}^2$ is the mean square electronic velocity averaged over all of the electrons. The trajectories for the equations (62) and (63) can be used to obtain electronic efficiencies for values of V_a/V_c different from 0.91 by terminating the trajectories at a radius different from R = 1 or at radius r_a. Thus, if the trajectories are

terminated at R = 0.88, V_a/V_c would be equal to 1. It is only necessary to take into account the fact that the normalizing factor is changed in the dimensionless variable R. Actual electronic efficiencies calculated for $V_a/V_c = 1$ were very low and could easily have been zero within the accuracy of the computations.

However, this situation is changed if the trajectories are terminated at R = 0.905. This value was taken for convenience in reading the computer curves. Actually, the efficiency changes slowly with a small change in the radius at which the trajectories are stopped. However, it was not possible to take the value of R much greater than 0.905 and remain within the capacity of the computer. At R = 0.905 the static voltage is

$$V_a' = \frac{.805}{.9} V_a = .894\, V_a$$

$$= .813\, V_c \qquad (65)$$

$$V_c' = (.905)^2 \frac{(1 - 1/81)^2}{(1 - 1/100)^2} V_c = .82\, V_c \qquad (66)$$

The static voltage at R = 0.905 is designated by V_a' and the cut-off voltage at R = 0.905 is designated by V_c'. Thus, from (65) and (66)

$$V_a' = .99\, V_c'$$

These calculations show that, for the anode radius assumed, the anode voltage is 99% of the cut-off voltage. Also the electronic efficiency is

$$\eta_e = 1 - \frac{m\bar{v}^2}{2eV_a'}$$

$$\eta_e = 1 - \frac{m r_a^2 \omega_L^2}{2 e V_a'}\left\{\left(\overline{\frac{dR}{d\tau}}\right)^2 + \left(R\ \overline{\frac{d\phi}{d\tau}}\right)^2\right\} \qquad (67)$$

where, as before, the bar signifies mean square values. Substituting for $mr_a^2\,\omega_L^2$ from equation (61) results in

$$\eta_e = 1 - \frac{V_c}{(1 - r_c^2/r_a^2)\,V_a'}\left\{\left(\overline{\frac{dR}{d\tau}}\right)^2 + \left(R\,\overline{\frac{d\phi}{d\tau}}\right)^2\right\}$$

$$\eta_e = 1 - 1.24\left\{\left(\overline{\frac{dR}{d\tau}}\right)^2 + \left(R\,\overline{\frac{d\phi}{d\tau}}\right)^2\right\} \qquad (68)$$

Figure 13 shows $\left\{\left(\frac{dR}{d\tau}\right)^2 + \left(R\,\frac{d\phi}{d\tau}\right)^2\right\}$ for values of α spaced 30° apart, for various values of B/B_0 and $NV_1/16V_c$. In each case the velocity contributed by radial motion is negligible. If an electron failed to get out of the interaction space in a reasonable time (within the capacity of the computer), or if it returned to the cathode, it does not appear on the plot. In no case did electrons return to the cathode with appreciable energy.

The REAC computations can only be considered as a qualitative indication of the actual behavior of the solutions to equations (62) and (63). The plots of Figure 13 are scattered and discontinuous because a small change in an electron orbit can make a large change

in the number of loops that the electron makes between cathode and anode; they do not represent inaccuracy of calculation.

A change in the phase angle of 30° may be sufficient to make a large difference in the energy exchange. The electronic efficiencies calculated on the graphs are based on equation (68), and the assumption that the number of electrons leaving the cathode is independent of phase angle α. Furthermore, while the presence of space charge is accounted for in the static voltage, space charge effects are not included in the rf voltages. The values of mean square velocity are shown, as are the electronic efficiencies under the various conditions. The ratio of the maximum ac voltage gradient to dc voltage gradient is also listed; this value is obtained by using equation (62) and the constants used for the computation. The dc gradient is given by

$$\frac{V_a}{2V_c}\left(1 + \frac{r_c}{r_a}\right)\left(1 - \frac{r_c^2}{r_a^2}\right)$$

The maximum ac gradient for the principal component of rotating wave is given by

$$\frac{NV_1}{16V_c}\left(1 - \frac{r_c^2}{r_a^2}\right)^2 R^{(N/2 - 1)}$$

Since the maximum values of E_{rac} and $E_{\phi ac}$ are the same, the ratio of the two gradients gives either $\frac{\max E_{rac}}{E_{dc}}$ or $\frac{\max E_{\phi ac}}{E_{dc}}$.

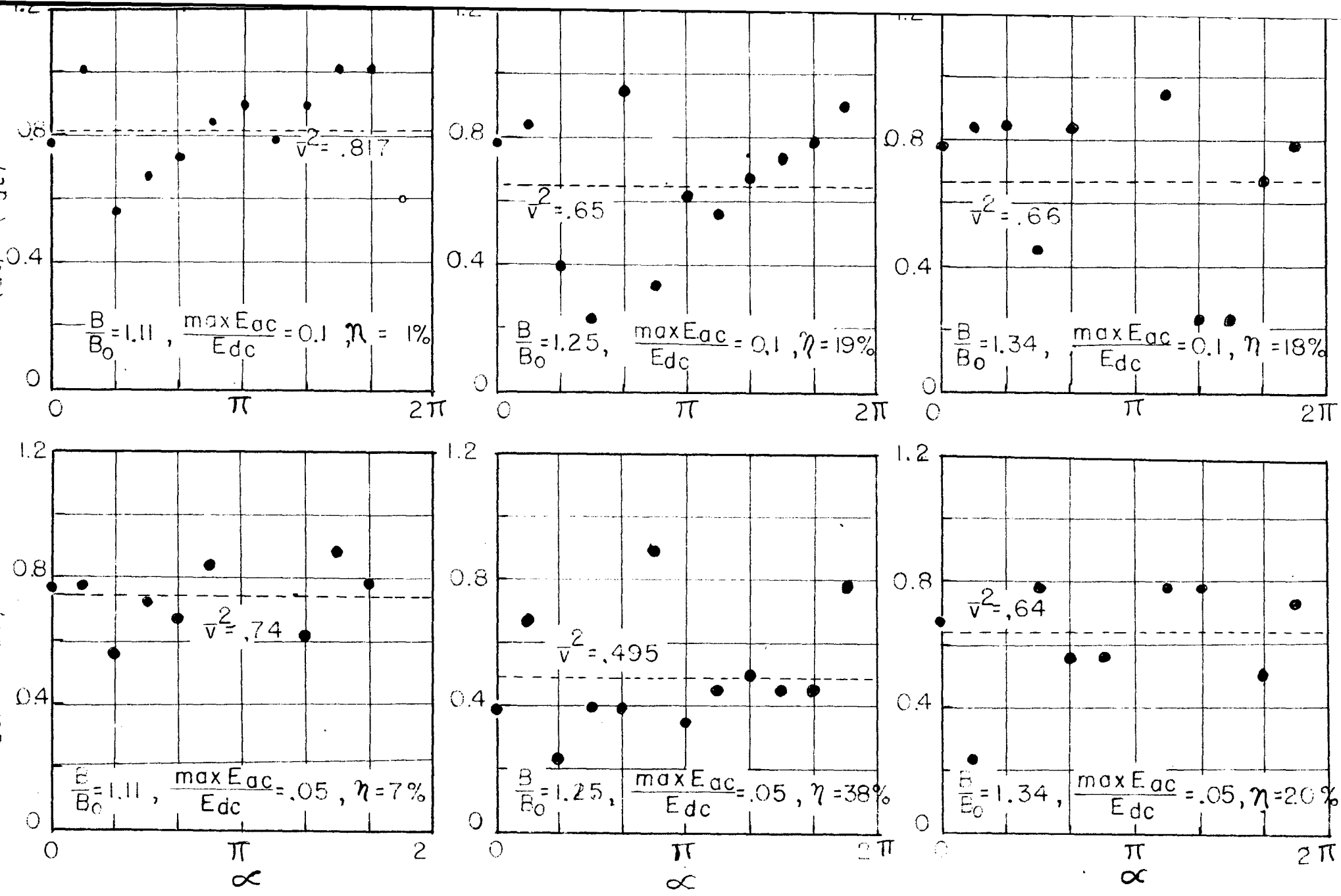

Figure 13

Relative velocities of electrons at anode for various phase angles.

In the computations, $\frac{V_a}{2V_c}\left(1+\frac{r_c}{r_a}\right)\left(1-\frac{r_c^2}{r_a^2}\right)$ was taken as 1/2; $\frac{NV_1}{16V_c}\left(1-\frac{r_c^2}{r_a^2}\right)^2$ had values of 0.2 and 0.4. At R = 0.905, this gives the approximate values of 0.05 and 0.1 for the ratios of max E_{ac}/E_{dc} for the respective cases. A value for $\frac{NV_1}{16V_c}\left(1-\frac{r_c^2}{r_a^2}\right)^2$ of 0.1 was also tried in the computations, but this field strength was so small that it was not possible to get even qualitative calculations. The effect on the trajectories was so slight that the electrons did not reach the anode in a reasonable time.

If it is supposed that the electrons have a mean square velocity equal to that of the traveling waves when they reach the anode, and that radial velocities are negligible, the efficiency can be calculated from

$$\eta = \frac{e V_a - e V_o}{e V_a} \quad . \tag{69}$$

In this equation, V_o is the characteristic voltage; and eV_o is the energy the electron must have to travel at the wave velocity. For the particular case of $V_a/V_c = 0.99$, and the values of 1.11, 1.25 and 1.34 for B/B_0, V_a is $0.99(B/B_0)^2$ or 1.22 V_o, 1.55 V_o and 1.77 V_o. These values correspond to efficiencies of 18%, 36% and 43%, as calculated from equation (69). For $B/B_0 = 1.25$, the maximum efficiency, as calculated from the trajectories, is the same within the accuracy of calculations obtained from equation (69). At

the higher and lower values of B, the efficiencies obtained from the trajectories is much less than that obtained from equation (69). This is because the extremely simple picture does not include the limitations placed on the allowable difference between the wave velocity and electron velocity, for proper interaction between the electrons and the wave.

The calculations give qualitative agreement with the concept of an electron stream traveling with velocity slightly greater than an rf wave delivering energy to the wave in a manner analogous to a traveling wave tube. The fields in a magnetron, however, are different from those in the traveling wave tube in that, in addition to a field component in the direction of travel E_ϕ, there is a transverse component E_r. Also, the situation is complicated by the fact that the static trajectories of the electrons are not in relatively uniform rf fields, as in the case of the traveling wave tube, but are alternately in strong and weak fields. To illustrate this fact, electron trajectories are shown for several values of α for $B/B_o = 1.25$ and $\frac{\max E_{ac}}{E_{dc}} = 0.05$ in Figures 14, 15 and 16.

Experimental Results

A series of experiments was undertaken to study the qualitative change which occurred when the size of the magnetron

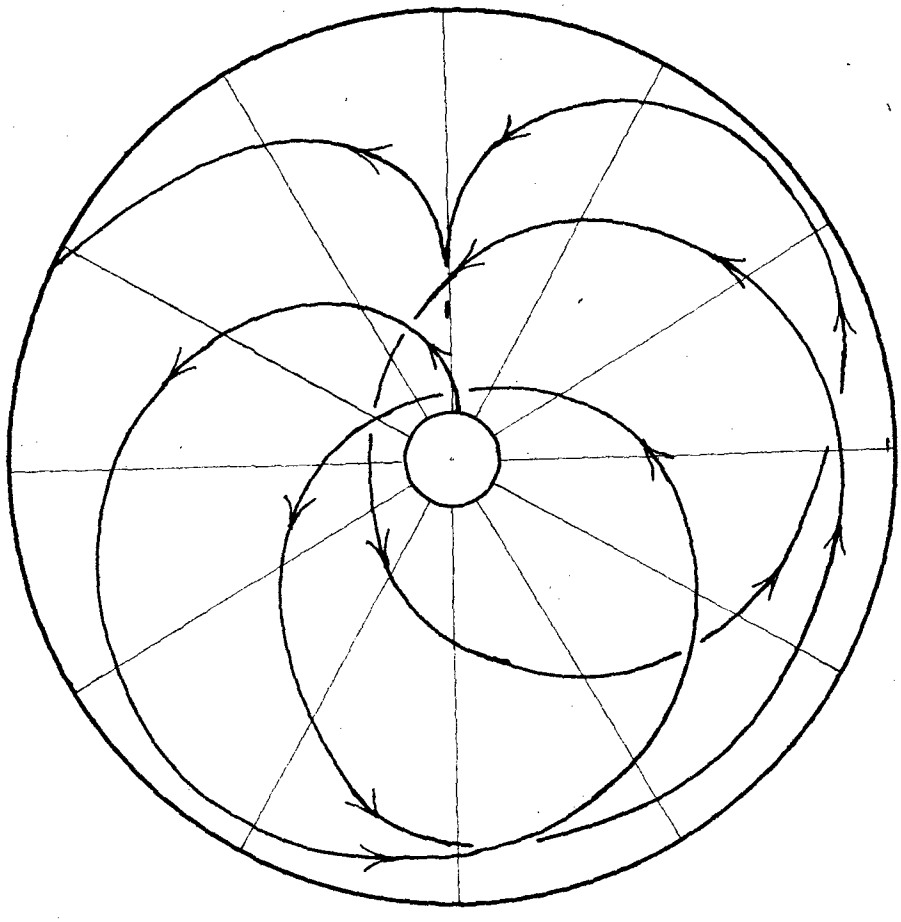

Electron trajectory for $B/B_0 = 1.25$,

$\frac{\max E_{ac}}{E_{dc}} = .05$, $\alpha = 0$

Figure 14

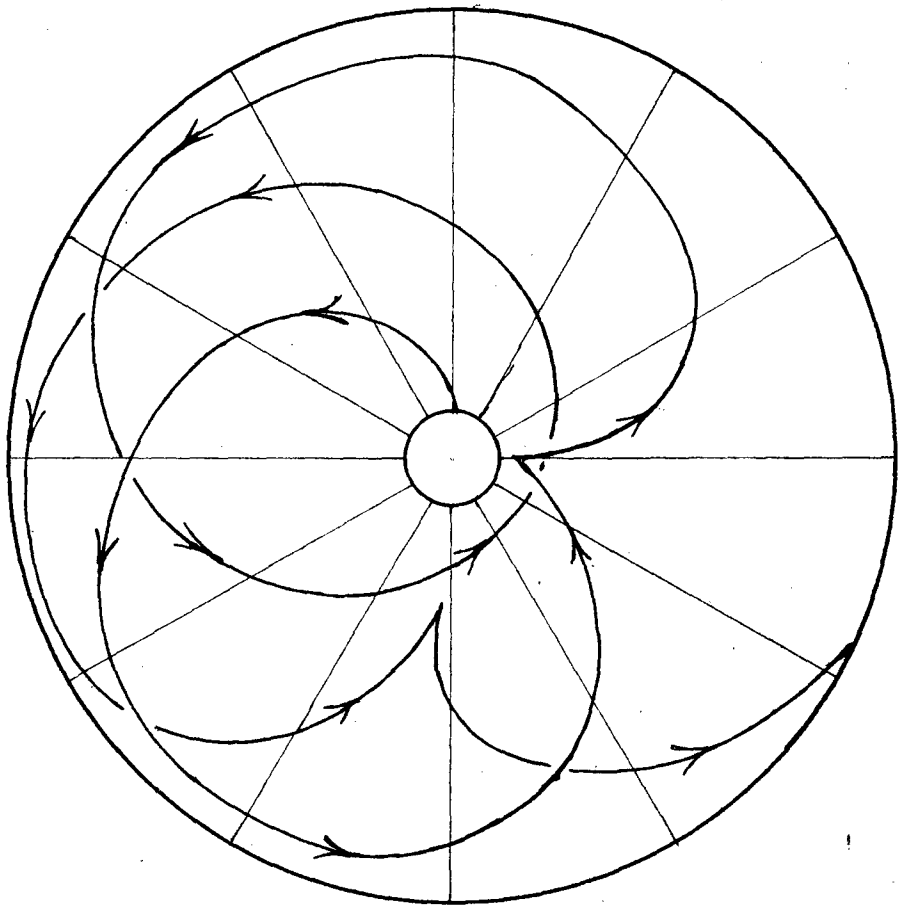

Electron trajectory for $B/B_0 = 1.25$,

$\frac{\max E_{ac}}{E_{dc}} = .05$, $\alpha = \frac{2\pi}{3}$

Figure 15

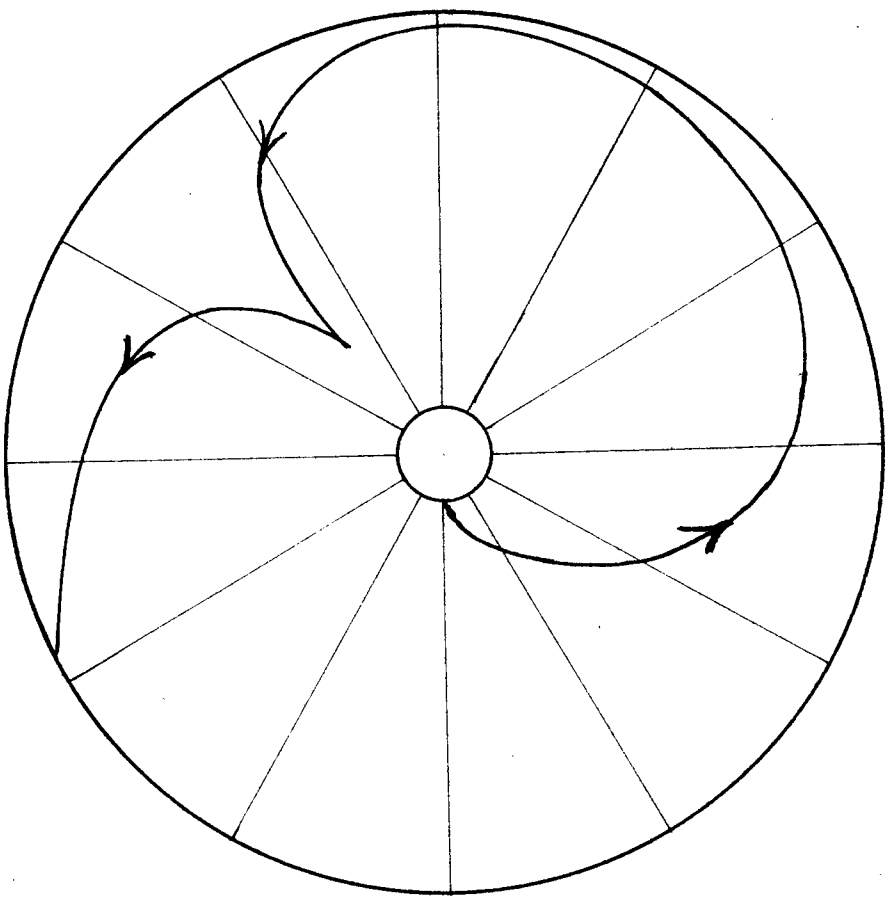

Electron trajectory for $B/B_0 = 1.25$,

$$\frac{\max E_{ac}}{E_{dc}} = .05 , \quad \alpha = \frac{4\pi}{3}$$

Figure 16

cathode was changed. It was found that as the cathode diameter was decreased, oscillations at low fields became more stable, within the capabilities of the cathode to emit. For small cathodes, the range of magnetic field over which the magnetron oscillates becomes finite. All of the tests were made with 18 vane rising sun anodes. The ratio of cathode to anode radius for normal operation as obtained from equation (26) is

$$r_c/r_a = 0.636 \ .$$

As this ratio is reduced from 0.636, stable oscillations are obtained at lower fields. The best power output and efficiency at low fields were obtained with r_c/r_a of the order of 0.1.

Tests were made to determine the relation of the region of oscillation to the Hartree line and the cut-off parabola. In Figures 17, 18 and 19, the shaded region is the oscillation region plotted in normalized coordinates, for different magnetron anodes. The cut-off curve is the one calculated from the theoretical relation. Since the currents used were of the order of 0.05 to 0.25 of the Langmuir current, it seems very unlikely that the oscillations actually occurred at voltages above the theoretical cut-off since the magnetron was operating space charge limited at the cathode. The experimental error inherent in the system was enough to shift this region by a sufficient amount to place it above the cut-off curve. In each case the range of magnetic field is approximately

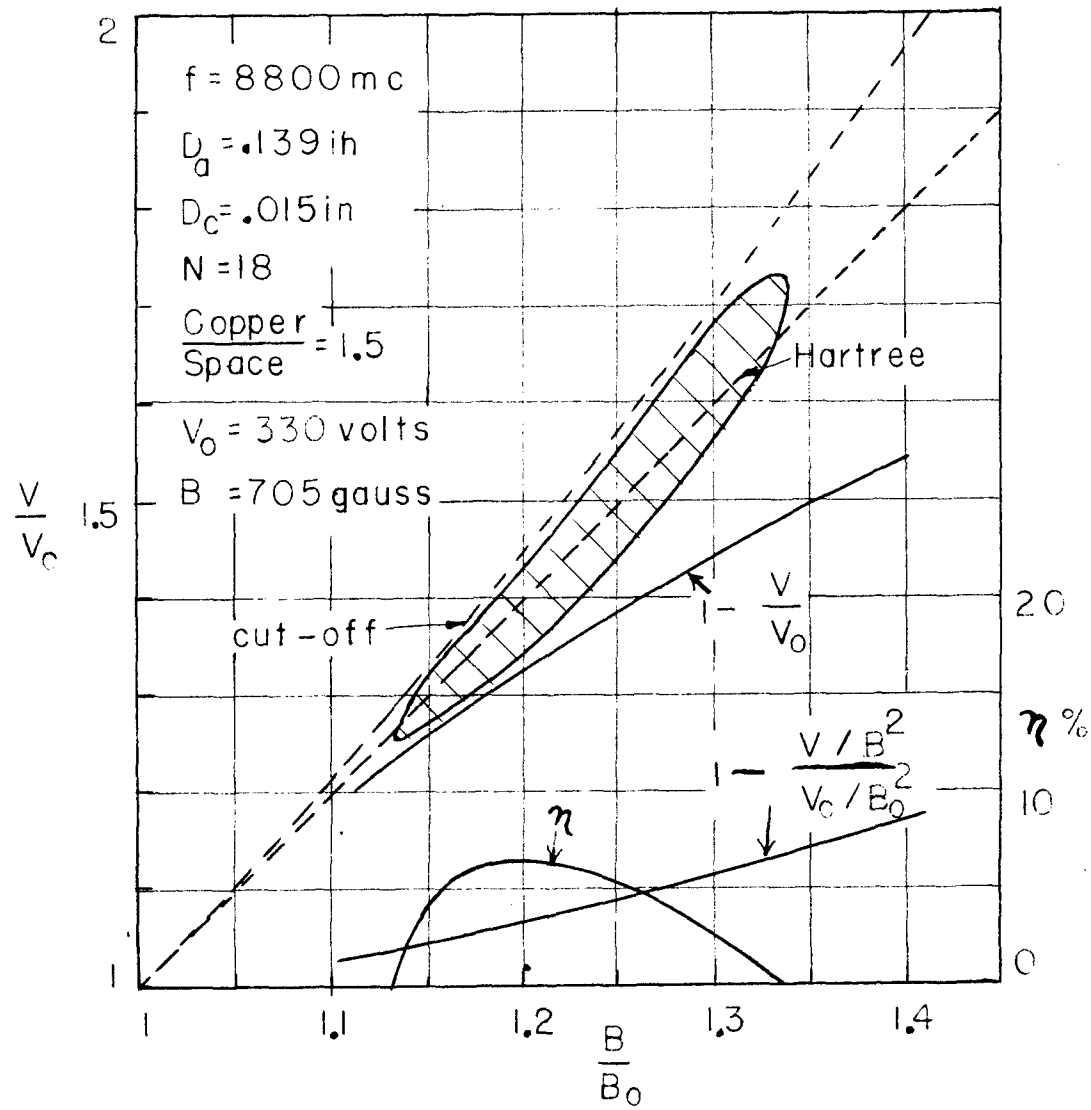

Figure 17

Region of oscillation and maximum overall efficiency η. The electronic efficiency is approximately twice the overall efficiency.

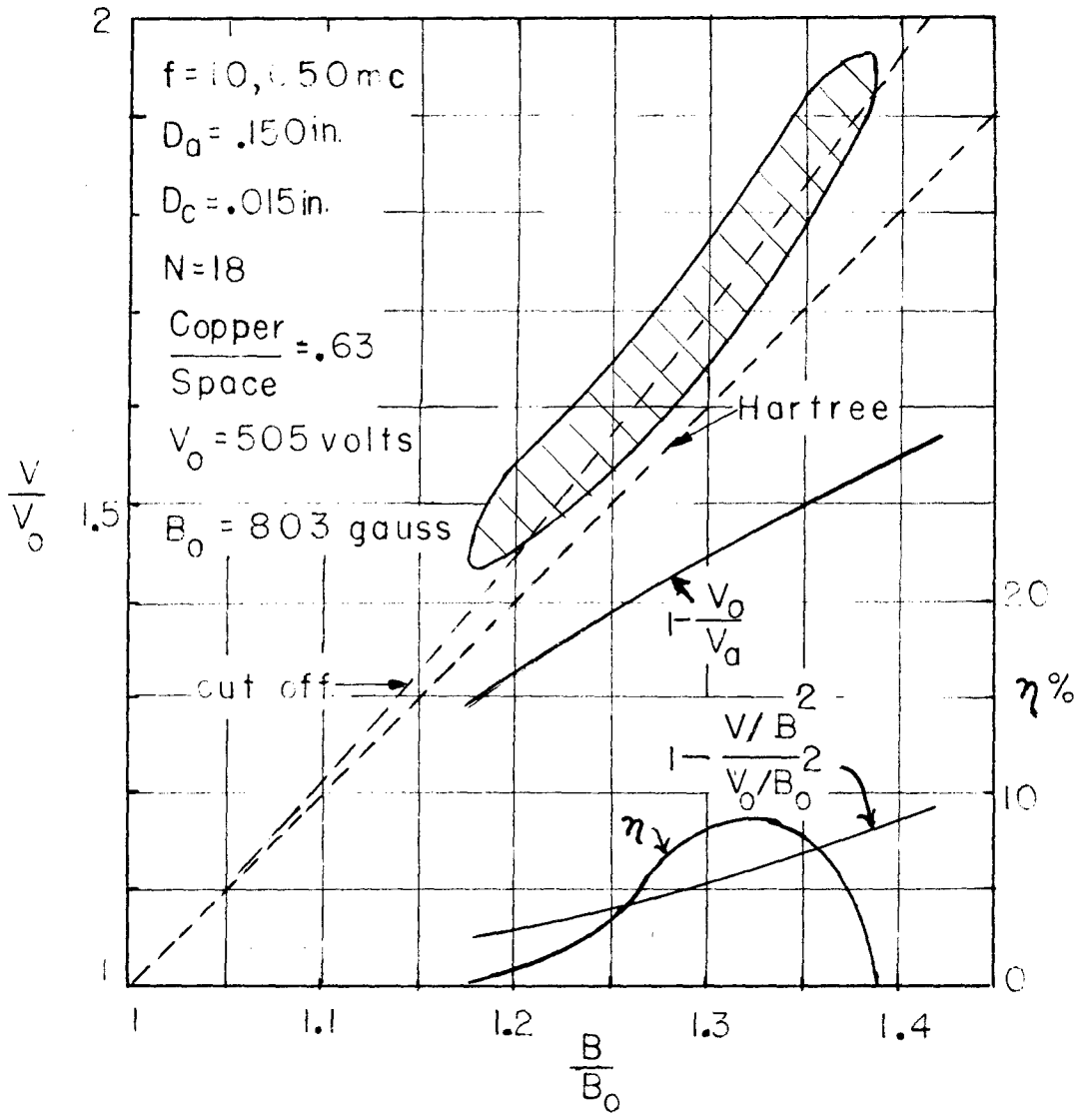

Figure 18

Region of oscillation and maximum overall efficiency η. The electronic efficiency is approximately twice the overall efficiency.

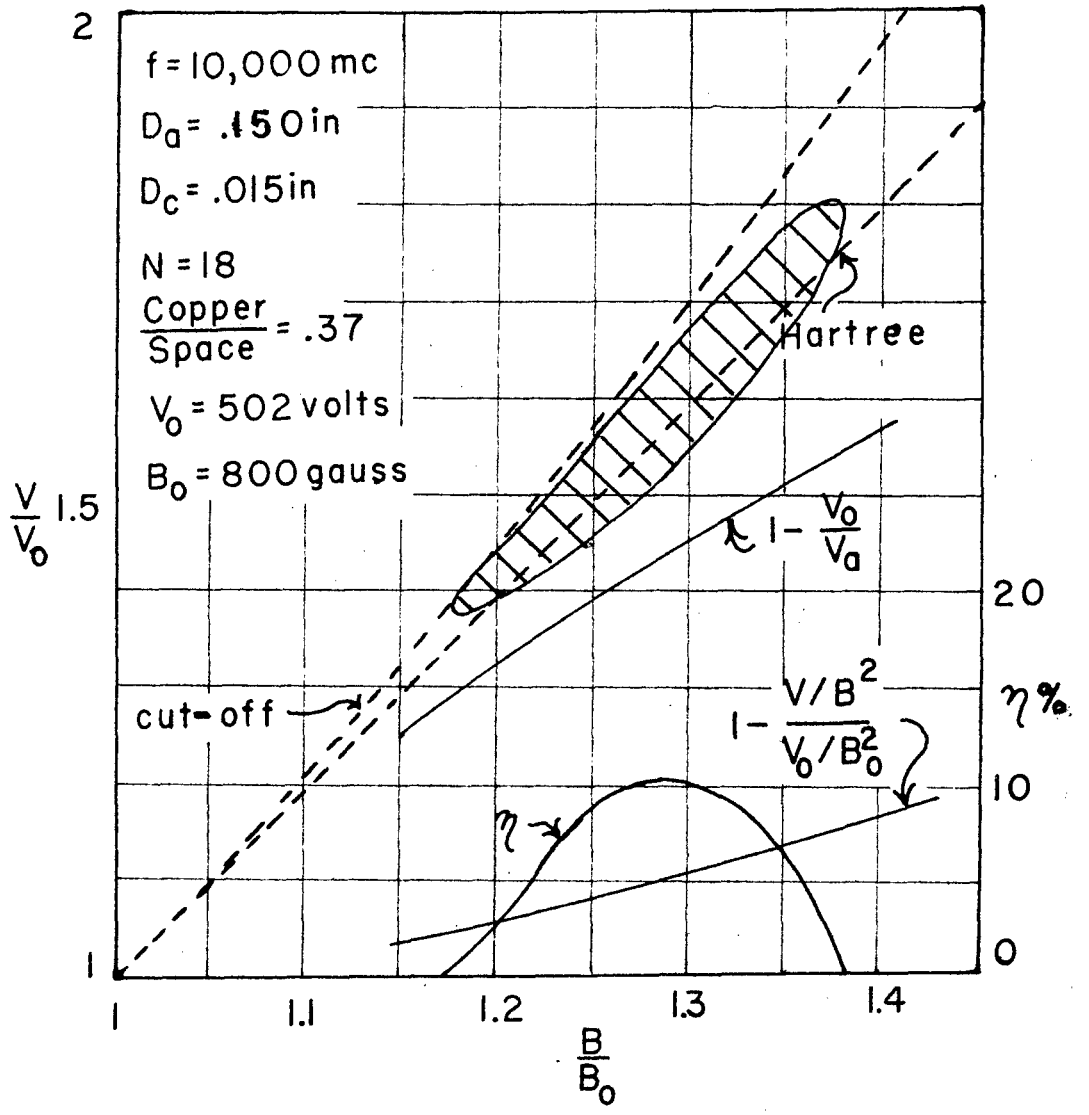

Figure 19

Region of oscillation and maximum overall efficiency η. The electronic efficiency is approximately twice the overall efficiency.

$$1.15 < B/B_0 < 1.40$$

Plots of maximum efficiency vs magnetic field are also shown in the figures. The maximum overall efficiency is of the order of 10%.

Magnetron theories predict that the efficiency of the magnetron goes to zero at $B = B_0$, $V = V_0$. However, these theories are usually extrapolated from approximations made at high field conditions and need not necessarily hold at low fields. The simplest of the "high field" theories requires that the electrons reach the anode with very nearly zero radial velocity and with angular velocity corresponding to V_0 volts. This results in a maximum value, as given by equation (69), for the electronic efficiency. For reference, this curve is plotted in the coordinates of Figures 17, 18 and 19. This theory certainly gives a larger value than is attainable since it neglects radial velocities and the velocity acquired by electrons which return to the cathode. It is very unlikely that the electrons would reach the anode with average velocity less than the wave velocity. A less optimistic theory -- that the electrons have acquired the maximum possible energy when they strike the anode[6] -- states

$$\eta = 1 - \frac{V/B^2}{V_0/B_0^2} \qquad (70)$$

This efficiency is also plotted on Figures 17, 18 and 19. We see that the actual efficiency obtained is somewhere between these two estimates. Rieke diagrams taken on all of the oscillators showed that the

magnetrons had very nearly their maximum efficiency when working into a matched load. Measurements of the Q's of the magnetrons showed that in each case the resonators were critically coupled to the load (i.e., $Q_0 = Q_e$) so that the maximum electronic efficiency is just twice the maximum overall efficiency. Thus, the actual electronic efficiency was comparable to the efficiency given by equation (69) and to that calculated from the trajectories.

The anodes had fin thickness ranging from 0.007 inches to 0.015 inches -- giving ratios of fin thickness to gap from 0.37 to 1.5. This is listed in Figures 17, 18 and 19 as copper/space ratio. The anode with the larger copper/space ratio worked at slightly lower fields, but it did not attain as high an efficiency as for the other cases. However, the electronic efficiency was comparable to that given by equation (69) at the particular fields where the magnetron oscillated best. Figures 20, 21 and 22 show a different aspect of the performance of the magnetrons where the power and efficiency is plotted in the V - I plane. In each case the maximum efficiency occurred at a current of about 0.2 of the Langmuir current calculated at the characteristic voltage V_0.

An attempt was made to operate a low field magnetron at higher voltage than was used in the 3 cm. tube. For this purpose, the anode diameter was held constant and the wavelength changed to 1.6 cm. In this case: N = 18; V_0 = 1,750 volts; B_0 = 1,500 gauss.

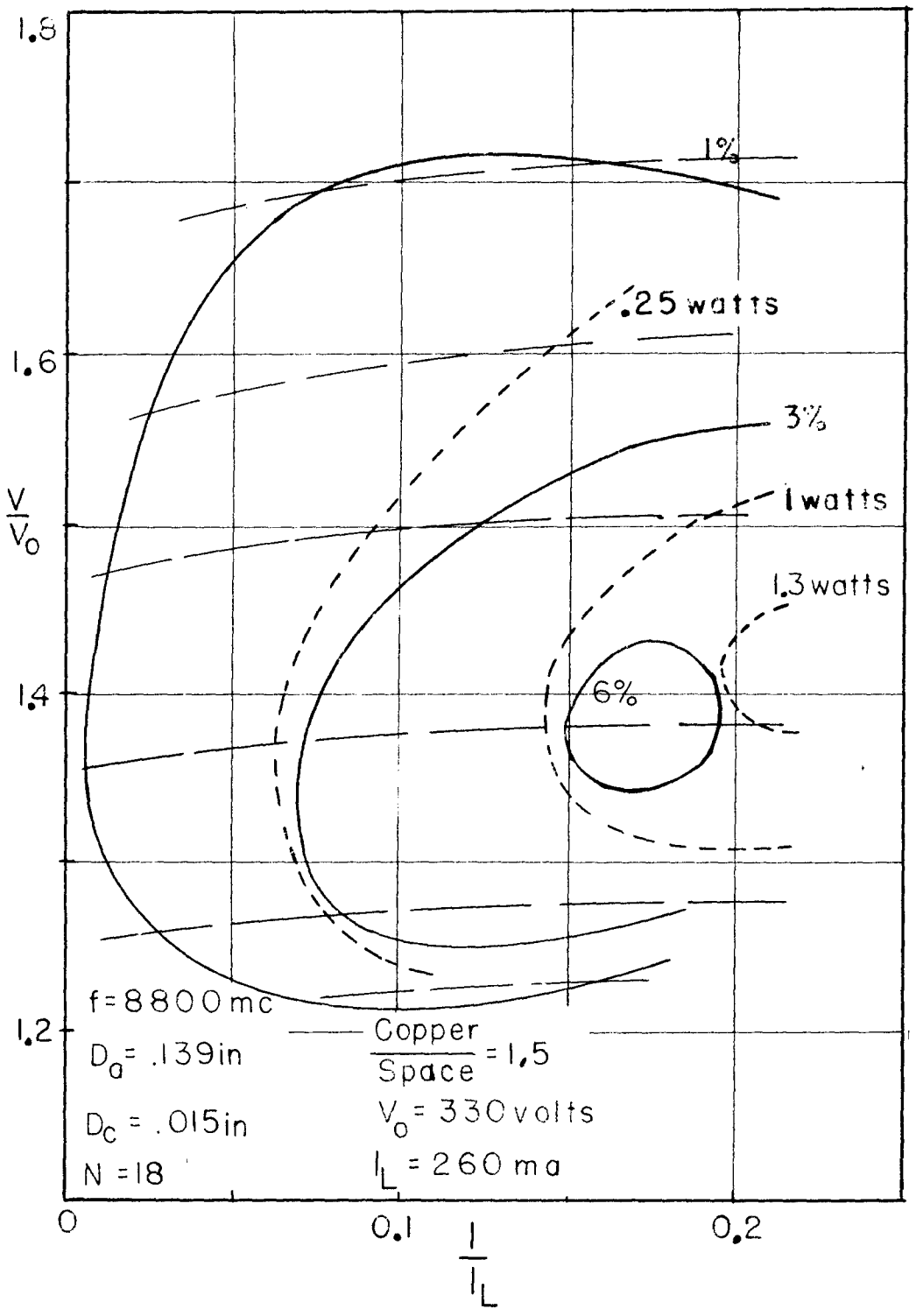

Figure 20

Normalized performance chart for low field magnetron.

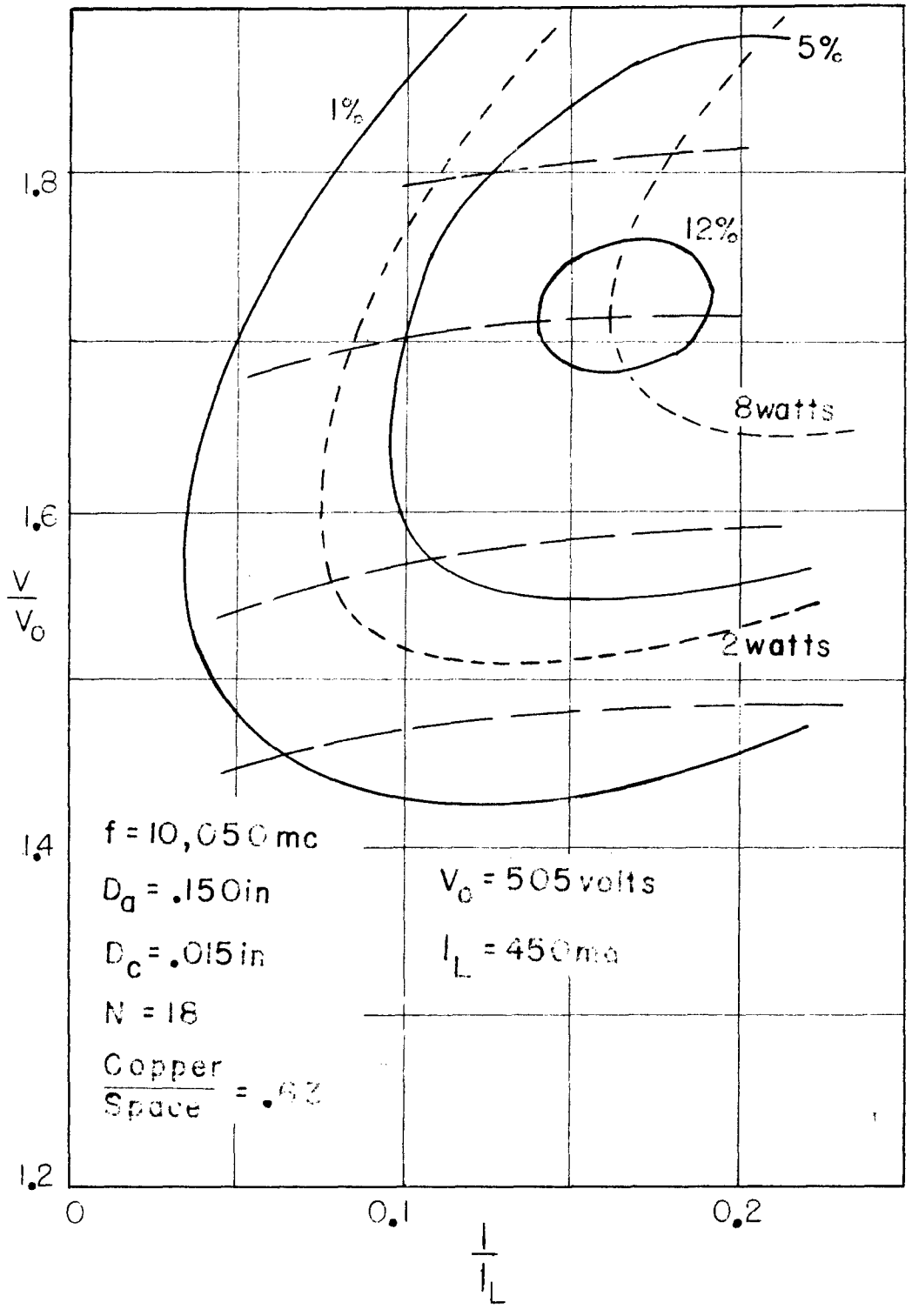

Figure 21

Normalized performance chart for low field magnetron.

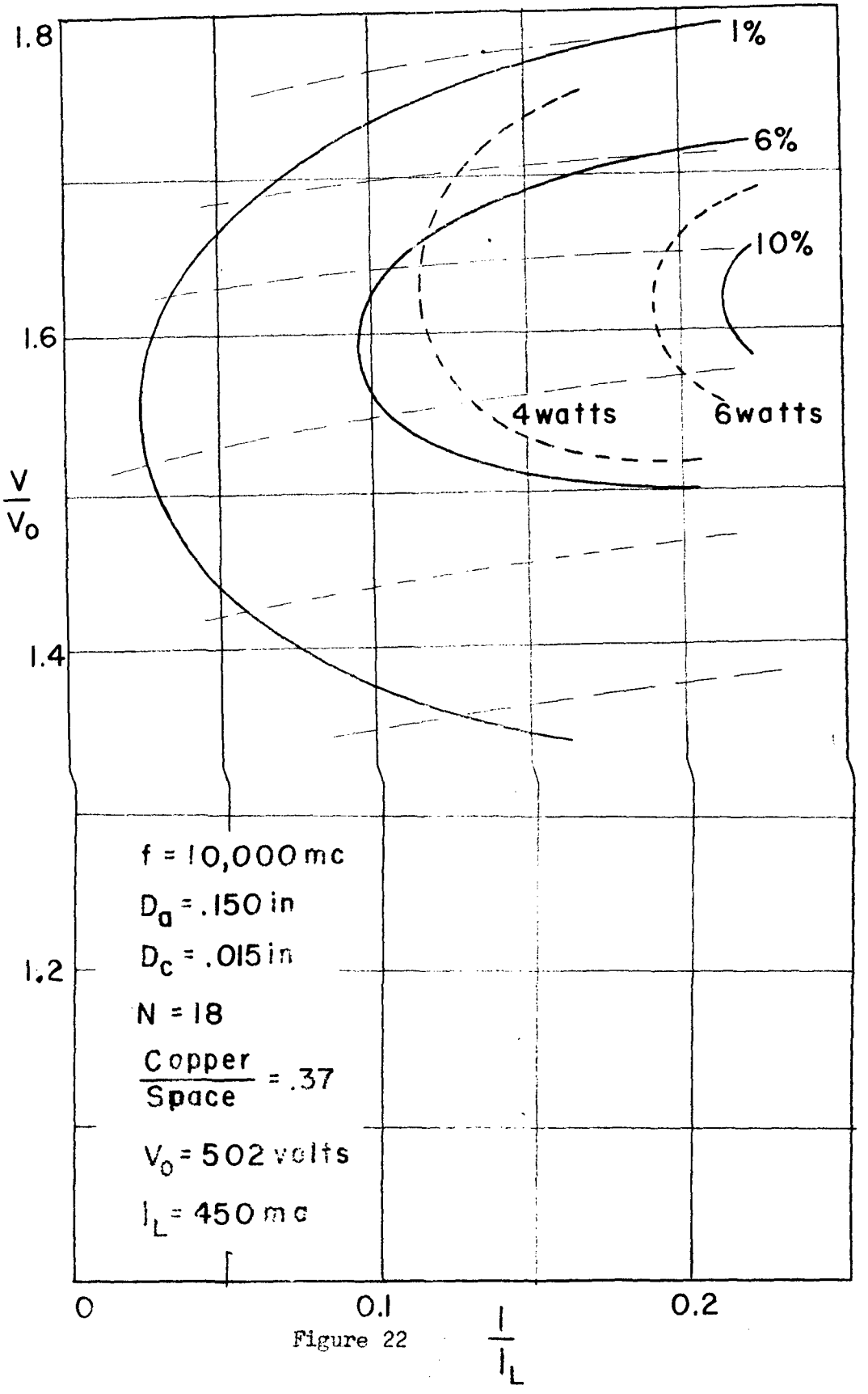

Figure 22

Normalized performance chart for low field magnetron

No power output data are available for this oscillator even though oscillations were obtained at the proper wavelength. A great deal of trouble was encountered with this magnetron because of the difficulty in obtaining a sharp cut-off curve. It was observed that the sharpness of the cut-off curve at voltages above 1,500 volts is a very critical function of the cathode centering. A set-up was built in which the cathode could be moved laterally during operation of the tube; and the position was set for the sharpest cut-off. It was observed while the tube was oscillating that the cathode position which corresponded to minimum current at a given voltage also corresponded to maximum intensity of oscillations. Furthermore, moving the cathode as much as 0.002 inches from the position of maximum intensity of oscillations completely stopped the tube from oscillating.

Back bombardment of the cathode was observed, but a more conclusive study would have to be made before anything can be said on this subject.

The degradation of the cut-off curve is much worse than would be calculated on the basis of small dimensional changes; the fact that small dimensional changes produced such a great change must be attributed to the setting up of ac fields when the cathode is moved slightly. (Long wavelength oscillations were observed under some circumstances when the magnetron was conducting below the Hull voltage.)

At cut-off voltages below 1,000 volts, the cut-off curve is not greatly affected by small changes in the position of the cathode. Also, the efficiency of operation of the oscillating magnetron is not critically dependent on cathode position, with a tolerance of about 0.003 in. to 0.005 in. on the axial alignment for good operation.

The voltage at which it is possible to operate a low field magnetron is limited by the violation of the Hull cut-off at high voltages. An estimate of the limitation of low field operation, therefore, depends on a more complete understanding of the violation of the Hull cut-off condition.

Another type of limitation which has not been studied is the effect of increasing the number N of resonators in the anode. The characteristic voltage V_0 is independent of the number N of resonators but dependent only on the distance from the center of one vane to the center of the next one. The characteristic magnetic field B_0, however, is a function of the number N. The characteristic voltage and magnetic field are related by the Hull cut-off equation

$$e V_0 = \frac{1}{2} m \left(\frac{B_0 e}{2m}\right)^2 r_a^2 \left(1 - \frac{r_c^2}{r_a^2}\right)^2 .$$

If V_0 is kept constant, but the number N of vanes is increased, the anode radius is proportional to N. Since the ratio r_c/r_a of cathode

to anode radius is not a function of N for low field operation, the characteristic magnetic field is proportional to the reciprocal of the anode radius (or to 1/N). Thus, it should be possible to operate with a smaller magnetic field as N is increased. The electronic operation, however, is certainly a function of N, the number of resonators, and this would have to be investigated before any predictions could safely be made.

CONCLUSIONS

The behavior of multiple circuit anode magnetron oscillators has been studied at the lowest possible electrical and magnetic fields. This type of magnetron operation affords very good possibilities of scaling into the millimeter region since the power input to a given size magnetron is relatively low.

The concept of the energy exchange at low fields, with small cathode radius, is that the electron cloud fills up almost the entire interaction space. The angular velocity of the electrons is 15% to 30% faster than the angular velocity of one of the rotating components of the rf standing wave. Under these conditions, the electrons lose energy to the traveling wave, allowing the tube to oscillate. This concept is in agreement with both experimental results and theoretical calculations. It is recommended that a study be undertaken to find the effect of increasing the number of resonators, and to find the largest possible cathode diameter that can be used. The first objective could be done with continuously pumped, demountable tubes; the demountable tube is not suitable for the second objective. The highest voltage at which it is possible to operate low field magnetrons is limited by the violation of the Hull cut-off at high voltages; it is doubtful if voltages greater than 3,000 volts could be used. At anode voltages much greater than 1000 volts, the cathode centering becomes very critical and must be adjusted while the tube is in operation. A

detailed study of high voltage limitations is not practical on the demountable system. A complete study of the limitations of low-field magnetron operation requires the building of sealed-off tubes.

APPENDIX I

Planar and Cylindrical Magnetic Diodes

The theoretical and experimental analysis of the static magnetron has engaged the attention of many workers as a necessary preliminary to understanding salient features of the oscillating magnetron. The simplest static magnetron from the theoretical point of view is the infinite planar magnetron. Unfortunately this is not true from the experimental point of view. It is possible to build finite planar magnetrons, but these are not the most useful forms. However, an analysis of the planar magnetron can give a basis for the more difficult case of the cylindrical magnetron. The orders of magnitude of the various effects, such as space charge and relativistic effects, in the planar magnetron should give an indication of the magnitude of these effects in the cylindrical case.

Electronic Motion, Space Charge and Cut-off in the Infinite Planar Magnetron, Classical Treatment

For this discussion, it will be assumed that the ideal infinite magnetron will be oriented so that the cathode and anode are parallel to the y-z plane; the cathode being situated at $x = 0$, and the anode at the plane $x = d$. The magnetic field will be taken in the z direction. It will be assumed that there is no variation of quantities except in the x direction. Newtonian mechanics will be used.

The fundamental equations governing the electronic motions are

$$m_o x'' = f_x = - e By' + e(dV/dx) \tag{71}$$

$$m_o y'' = f_y = e Bx' \tag{72}$$

The symbols have the following definitions:

m_o equals the rest mass of the electron;

f_x and f_y denote the forces in the x and y directions respectively;

e equals the absolute value of the electronic charge (coulombs) (e is to be taken as a positive number);

B equals magnetic flux density (Webers/sq. meter);

V equals voltage difference in volts.

All distances are measured in meters. The ' symbol indicates differentiation with respect to time.

It will be assumed that the electrons leave the cathode with zero velocity. With this understanding, integration of (72) yields

$$m_o y' = e Bx \tag{73}$$

which, substituted into (71), results in

$$m_o x'' = - e B (e Bx/m_o) + e (dV/dx) \tag{74}$$

This equation is integrable, using x' as integrating factor. The result, using the convention that the voltage at the cathode is zero, is

$$1/2 (x')^2 = - (e B/m_o)^2 (x^2/2) + (e/m_o) V \tag{75}$$

It is interesting to note that this equation was obtained without a knowledge of the actual voltage distribution between the cathode

and point x. For this reason, the cut-off relation in the non-relativistic, or classical, treatment is independent of the presence of space charge. This is not the case for the relativistic treatment. The cut-off relation is obtained by supposing that the x velocity is zero at the anode (x = d). The substitution of this relation into (75) gives the cut-off relation

$$e/m_o V_c = (eB/m_o)^2 d^2/2 \qquad (76)$$

where V_c is the cut off voltage Hereafter V_c will be used to designate the cut off voltage as calculated by the non-relativistic mechanics.

A detailed treatment of the actual variation of V with x in the presence of space charge, and of the trajectories of the electrons, requires the imposition of the divergence relation and the equation of continuity of charge. These relations are:

$$\text{Div } D = \rho \qquad \text{(divergence relation)} \qquad (77)$$

$$\text{Div } J = 0 \qquad \text{(continuity of charge)} \qquad (78)$$

In these equations D equals electric flux density, ρ equals space charge density, and J equals total current density. For the case of static fields, J is the convection current density and is given by

$$J = \rho v \qquad (79)$$

where v is the vector velocity. For the case of variation of quantities only in the x-direction, (77) becomes

$$- \epsilon \, d^2V/dx^2 = \rho \qquad (80)$$

where ϵ is the dielectric constant of space. Similarly, (78) becomes

$$J_x = \text{const.} \qquad (81)$$

The substitution of the divergence and continuity relations into (79) results in

$$J_x = - \epsilon \, (d^2V/dx^2) \, x' \qquad (82)$$

where x' is the velocity of the electrons at the x-plane. If x is interpreted as the position of the electron at time t, and V as the voltage through which the electron has fallen in time t, (82) integrates to

$$J_x \, t = - \epsilon \, dV/dx \qquad (83)$$

where it is assumed that the voltage gradient is zero at $x = 0$. (Assume space charge limitation, neglecting initial velocities.)

The substitution of (83) into (74) yields a differential equation for the x directed motion of the electrons in the presence of space charge. This equation is

$$x'' = - (e B/m_o)^2 \, x - (e/\epsilon m_o) \, J_x t \quad . \qquad (84)$$

This equation is easily integrable, and has the general solution

$$x = C_1 \cos \omega_o \, t + C_2 \sin \omega_o \, t - \frac{J_x \, m_o \, t}{\epsilon e \, B^2} \qquad (85)$$

where ω_o is the cyclotron frequency, eB/m_o. It should be noted that J_x is a negative number in these equations. The initial conditions are that at $t = 0$, $x = 0$ and $x' = 0$ so that $C_1 = 0$ and C_2

$= J_x/(\in B\, \omega_o^2)$. The resulting equation for x is

$$x = - \frac{J_x}{\in B\, \omega_o} \left(t - \frac{\sin \omega_o t}{\omega_o}\right) . \qquad (86)$$

The y-directed velocity and the y-position are obtained by substituting (86) into (73). It is assumed that y is zero at t = 0.

$$y' = (eB/m_o)\, x \qquad (87)$$

$$y = (- J_x/ \in B) \left\{ t^2/2 + \frac{\cos \omega_o t - 1}{\omega_o^2} \right\} \qquad (88)$$

The voltage at time t is obtained from conservation of energy. Thus

$$V = \frac{1}{2} \frac{m}{e} \left\{ \omega_o^2\, x^2 + \frac{J_x^2}{\in^2 \omega_o^2 B^2} (1 - \cos \omega_o t)^2 \right\} \qquad (89)$$

The equations will be reduced to dimensionless variables to obtain a better picture of their significance. Let

$$\beta = \frac{V - V_c\, (x^2/d^2)}{V_c} \qquad (90)$$

where V_c is the cut-off voltage as calculated in (76) . At x = d, β has the physical significance of being the percentage increase of the anode voltage above the cut-off voltage. Let

$$\alpha = J_x/J_L \qquad (91)$$

where J_L is the space-charge-limited current density that would exist if the voltage V_c were applied to the anode in the absence of magnetic field.

$$J_L = -\frac{4\epsilon}{9}\sqrt{\frac{2e}{m_o}}\ \frac{(V_c)^{3/2}}{d^2} \qquad (92)$$

The substitution of these variables into (86), (88) and (89), with algebraic simplification using (76) and (92) yields

$$x/d = 2\alpha/9\ (\omega_o t - \sin \omega_o t) \qquad (93)$$

$$y/d = 2\alpha/9 \left\{ \frac{(\omega_o t)^2}{2} + \cos \omega_o t - 1 \right\} \qquad (94)$$

$$\beta = 4\alpha^2/81\ (1 - \cos \omega_o t)^2 \ . \qquad (95)$$

Equations (93) and (94) are the parametric equations of the electron trajectories. Equation (95) gives the voltage at any point along the trajectory. These equations were derived on the stringent assumption of single velocities at a given plane. As will be seen later, this assumption is very questionable at low currents.

If, in equations (93) and (95), the substitutions are made that $x = d$, $\omega_o t = \omega_o t_a = \theta$ where t_a is the time of transit from the cathode to the anode, the resulting equations are parametric relations between β and α. This relation is the current-voltage cut-off curve, and can be written

$$\beta = 4\alpha^2/81\ (1 - \cos \theta)^2 \qquad (96)$$

$$1 = 2\alpha/9\ (\theta - \sin \theta)^2 \ .$$

Figure 23 is a plot of β vs α. At $\alpha = 9/(4\pi)$, $\beta = 0$ and for values of $\alpha > 9/(4\pi)$ the curve approaches the Langmuir current (the current which would flow if there were no magnetic field). As

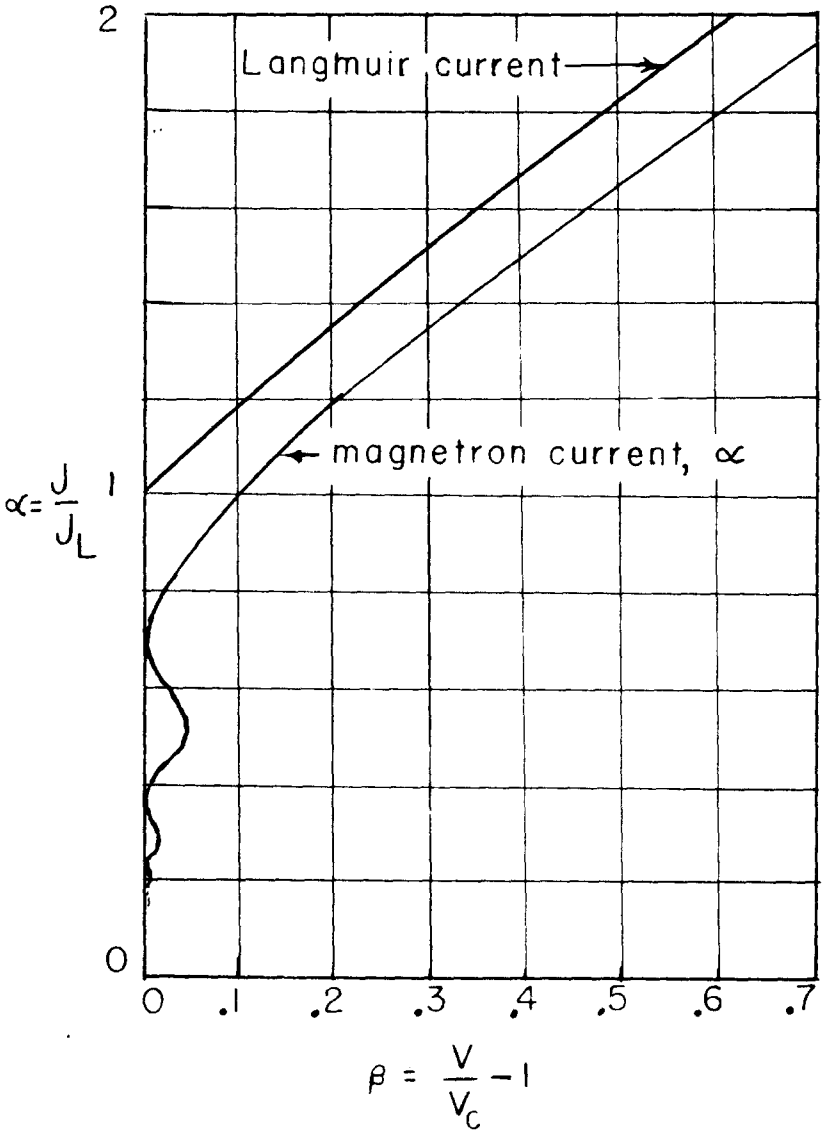

Figure 23

$\propto$ as a function of β

α approaches zero, θ approaches infinity and the curve of β vs α oscillates back and forth, touching the line $\beta = 0$ at values of $\theta = 2n\pi$ where n is a positive integer, and reaching maxima at θ equal to $(2n + 1)\pi$ where n is, as before, a positive integer. The first several maxima and zeros of β are tabulated in decreasing magnitudes of α.

n	α	β
1	.715	0
1	.48	.045
2	.358	0
2	.286	.0162
3	.239	0
3	.204	.0083

It is seen that the zeros and maxima are interlaced. As far as the writer knows, this oscillation of the voltage in the uncut-off magnetron has never been observed. However, some writers imply that this oscillation in the V - I curve is responsible for negative resistance in the electron stream.(7)

The present calculation has been made for the planar magnetron, but its behavior should be essentially the same as the cylindrical magnetron with cathode and anode radii very nearly the same.

It is of interest to calculate the space charge density in the electron stream. Equations (93) and (95)may be used as parametric equations relating V and x. Solving (90) for V one obtains

$$V = V_c \left\{ \frac{x^2}{d^2} + \beta \right\} \quad . \tag{98}$$

Substitution into (80) gives the space charge density

$$\rho = \frac{- \epsilon (m_o/e) \omega_o^2}{1 - \cos \omega_o t} \quad . \tag{99}$$

Thus, at the values of t where $\omega_o t = 2n\pi$, the elctron passes through regions where the charge density is infinite. At these same planes, the x directed velocity becomes zero.

The mechanics which has been used is reversible, so that an electron could either proceed on out to the anode from one of the space charge "striations," or it could reverse its direction and return to the cathode. In the plot of β vs α, β is zero (or the anode voltage is equal to V_c) for any current which places a space-charge striation at the anode. For any current corresponding to $\alpha > .715$, V is greater than V_c. It is possible to set up a solution for $\alpha < .715$ with V equal to V_c by assuming a double stream. For example, let it be assumed that the transit angle from the cathode to the anode is $\omega_o t_a = 2\pi$, and that no matter what the current, the numerical sum of the currents in the two streams is $.715 J_L$. This would automatically satisfy the divergence relation, giving the proper voltage distribution. Then to get the appropriate net anode current, all that is necessary is to make the difference of the two currents equal the net flow. In this way it is possible to set up an infinite variety of solutions in the cathode-anode region -- all of which satisfy the macroscopic electrodynamical equations.

In many cases, two or more very different space charge configurations give the same anode voltage and current.

Symmetrical States for the Cylindrical Magnetron

In order to obtain an understanding of the static conditions in the cylindrical magnetron, the analogue of the calculations for the planar case will be carried out. The divergence and continuity equations are

$$\frac{\partial D_r}{\partial r} + \frac{1}{r} D_r = \rho \quad , \tag{100}$$

$$I_r = 2\pi r \rho \, (dr/dt) = \begin{array}{l}\text{current per} \\ \text{unit length}\end{array} . \tag{101}$$

The current I_r is a constant. All variables are to be considered as functions of time t for an electron that leaves the cathode at $t = 0$. By eliminating ρ from equations (100) and (101), and using the definition of D_r, one obtains

$$\left\{ r \frac{d^2V}{dr^2} + \frac{dV}{dr} \right\} \frac{dr}{dt} = - \frac{I_r}{2\pi \epsilon} . \tag{102}$$

Integration of (102) yields

$$r \frac{dV}{dr} = - \frac{I_r t}{2\pi \epsilon} . \tag{103}$$

The initial conditions are that at $t = 0$, the electron is at the cathode where space-charge limited conditions exist so that $dV/dr = 0$ at $t = 0$. The equations of motion for the electron in the symmetrical state are

$$(d/dt)\left(r^2\ (d\phi/dt)\right) = (Ber/m)\,(dr/dt) \qquad (104)$$

and

$$d^2r/dt^2 - r\ (d\phi/dt)^2 = (e/m)\,(dV/dr) - (Be/m)\ r\,(d\phi/dt). \qquad (105)$$

In these equations, B is the axial magnetic field. Integration of (104) yields

$$r^2\ (d\phi/dt) = (Be/2m)(r^2 - r_c^2) \quad . \qquad (106)$$

The initial conditions for this equation are that the velocity, and therefore $d\phi/dt$, is zero at $r = r_c$, the cathode radius. The Hull cut-off voltage can be obtained if it is assumed that the electrons have zero radial velocity at the anode. Designate the cut-off voltage as V_c, then

$$eV_c = 1/2\ m\ (r_a\ d\phi/dt)^2 \qquad (107)$$

or

$$V_c = (m/2e)\ (Be/2m)^2\ r_a^2\ \ (1 - r_c^2/r_a^2\ )^2 \quad . \qquad (108)$$

Substitution of equations (103) and (106) into the equation for radial acceleration, (105), results in

$$(d^2r/dt^2) + (Be/2m)^2\ r - (Be/2m)^2\ (r_c^4/r^3) = -\frac{I_r\ e\ t}{2\pi \in r\ m} \quad . \qquad (109)$$

This is the differential equation for the radius r of an electron starting out at the cathode at $t = 0$, with a radial current I_r, and includes the effect of space charge. Introduction of dimensionless variables results in further simplification. Let

$$S = r/r_c \tag{110}$$

$$\tau = (Be/2m)\, t \tag{111}$$

$$\omega_L = Be/2m \tag{112}$$

The angular frequency ω_L is the Larmor frequency. Equation (109) becomes

$$\frac{d^2S}{dt^2} + S - \frac{1}{S^3} = - \frac{I_r\, e\, \tau}{2\pi \in r_c^2\, \omega_L^3\, m\, S} . \tag{113}$$

The constant in the right hand term of equation (113) can be expressed in terms of the Langmuir current, or space-charge-limited current which would flow in the absence of magnetic field, with cut-off voltage applied to the anode. In equation (113) I_r is a negative number. In keeping with this convention, the Langmuir current will also be taken as a negative number, so that

$$I_L = - \in \frac{8\sqrt{2}\,\pi}{9\beta^2} \sqrt{\frac{e}{m}}\, \frac{V_c^{3/2}}{r_a} \tag{114}$$

In this equation, β is a dimensionless variable, which is a function of r_c/r_a, and is tabulated by Langmuir. Using the cut-off relation (107) and equation (114) to eliminate ω_L from equation (113) results in

$$\frac{d^2S}{d\tau^2} + S - \frac{1}{S^3} = \frac{r_a^2}{r_c^2} \left(1 - \frac{r_c^2}{r_a^2} \right) \frac{8}{36\beta^2}\, \frac{I_r}{I_L}\, \frac{\tau}{S} \tag{115}$$

Equation (115) may be written as

$$d^2S/d\tau^2 + S - 1/S^3 = K\,(\tau/S) \tag{116}$$

where

$$K = \frac{r_a^2}{r_c^2}\left(1 - \frac{r_c^2}{r_a^2}\right)\frac{8}{36\beta^2}\frac{I_r}{I_L} \qquad (127)$$

The graphs in Figure 24 shows solutions plotted for K ranging from 1.6 to 16. These solutions were obtained using the REAC analogue. computer. It is characteristic of all of these solutions that at the first zero of $dS/d\tau$, not counting the one at $\tau = 0$, $dS/d\tau$ becomes negative. The calculation has no physical significance for τ greater than this value. The situation is not so simple for smaller values of K ($K < 1.6$). For values of $K < 1.6$, the graph of $dS/d\tau$ vs τ changes its nature, $dS/d\tau$ no longer becoming negative at its first zero ($\tau \neq 0$). When $dS/d\tau$ becomes zero, but does not become negative, there is the possibility of more than one space charge striation. Calculations of Hartree,[8][9] Allis, etc., indicate that space charge striations are possible for values of S up to about two and one-half. There is no self consistent solution which allows more than one striation, and which has a striation at a normalized rasius greater than two and one-half. The smallest current at which a single stream solution which has just one striation is possible is called the Allis current, and is usually about 3/4 of the Langmuir current. This current places a space charge striation at the anode.

These considerations lead to the conclusion that for the static magnetron, with $r_a/r_c > 2.5$, operating at the cut-off voltage with

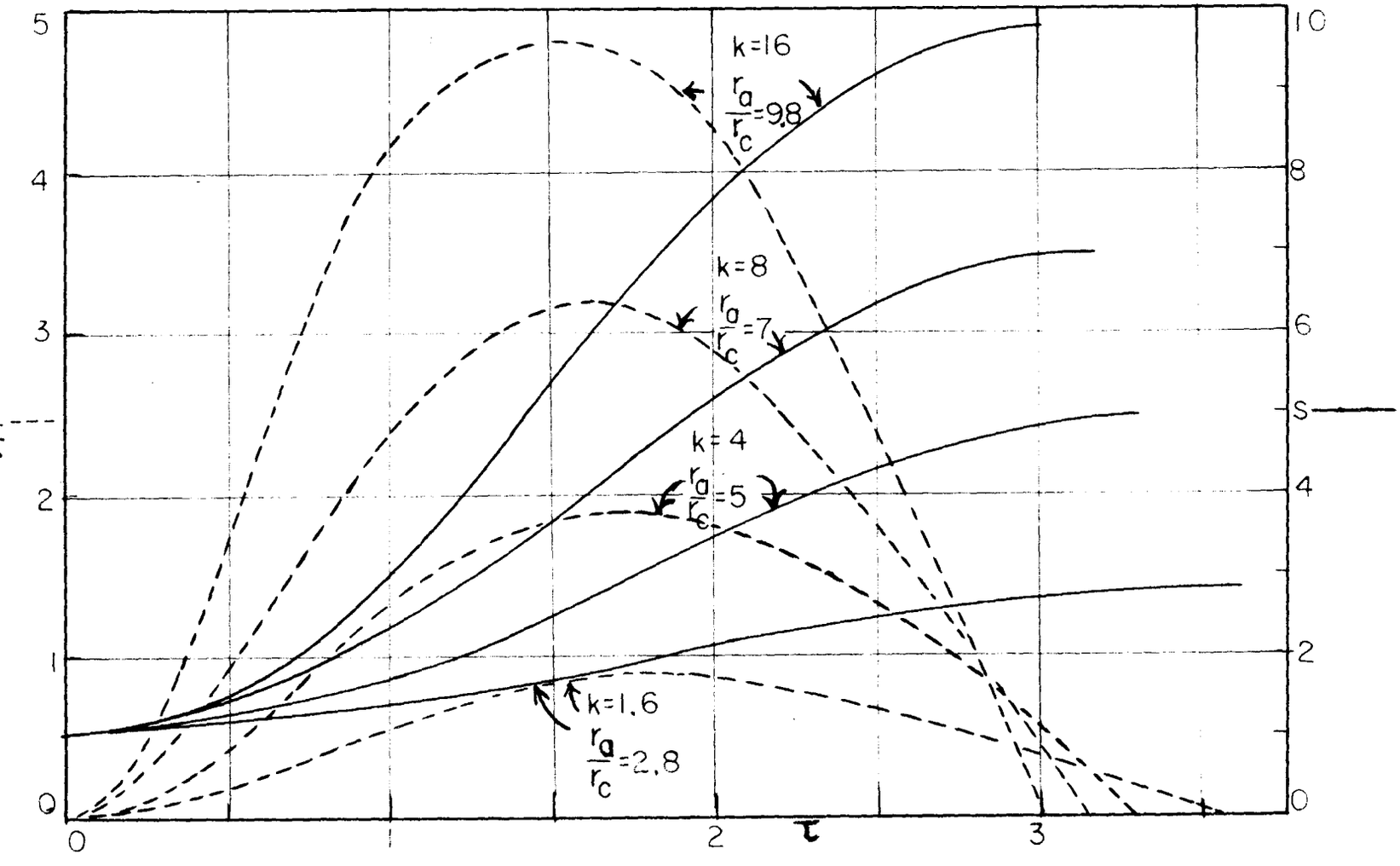

Figure 24

Normalized electron radii and velocity as a function of normalized time.

space-charge limited current less than the Allis current there must be a double stream of electrons. The arithmetical sum of the currents in the double stream is equal to the Allis current, so that the potential distribution is the same as if the magnetron were operating at the Allis current The difference of the two currents gives the net current flowing to the anode. This simple picture of the behavior of the static magnetron does not explain conduction of current at voltages below the cut-off, as found by Jepsen.[10] However, it seems reasonable to suppose that for currents that are a fairly large percentage of the Allis current (and voltages at cut-off voltage) the theoretical interpretation is fairly complete. Low field magnetron oscillations have been observed at currents of about 0.05 to 0.25 of the Langmuir current. It should be pointed out that there exists the possibility of a single stream solution in which the electrons rotate in circular orbits around the cathode for the magnetron at cut-off. This solution does not allow radial flow of current, however.

Electron Trajectories and Voltage Distribution

In terms of the dimensionless variables τ and S, the equation (106) for angular velocity is

$$d\phi/d\tau = (1 - 1/S^2) \tag{118}$$

$$\phi = \tau - \int_0^{\tau} d\tau/S^2 \tag{119}$$

Using the solutions for S, it is possible to obtain the electron trajectories by evaluating the integral in equation (119) . Figure 25 shows trajectories for $r_a/r_c = 2.5$, 5, and 9.8.

The voltage at a given radius is given by

$$eV = \frac{1}{2} m \left\{ \left(\frac{dr}{dt} \right)^2 + r^2 \left(\frac{d\phi}{dt} \right)^2 \right\} \tag{120}$$

Substitution of dimensionless variables into (120) results in

$$eV = \frac{1}{2} m r_c^2 \omega_L^2 \left\{ \left(\frac{dS}{d\tau} \right)^2 + S^2 \left(\frac{d\phi}{d\tau} \right)^2 \right\} \tag{121}$$

Dividing this equation by the cut-off relation (107) and substituting for $(d\theta/d\tau)$ from (118) yields

$$\frac{V}{V_c} = \frac{r_c^2}{r_a^2 \left(1 - r_c^2/r_a^2\right)^2} \left\{ \left(\frac{dS}{d\tau} \right)^2 + S^2 \left(1 - \frac{1}{S^2} \right)^2 \right\} \tag{122}$$

Figures 26 and 27 show V/V_c as a function of S for $r_a/r_c = 2.8$ and 9.8.

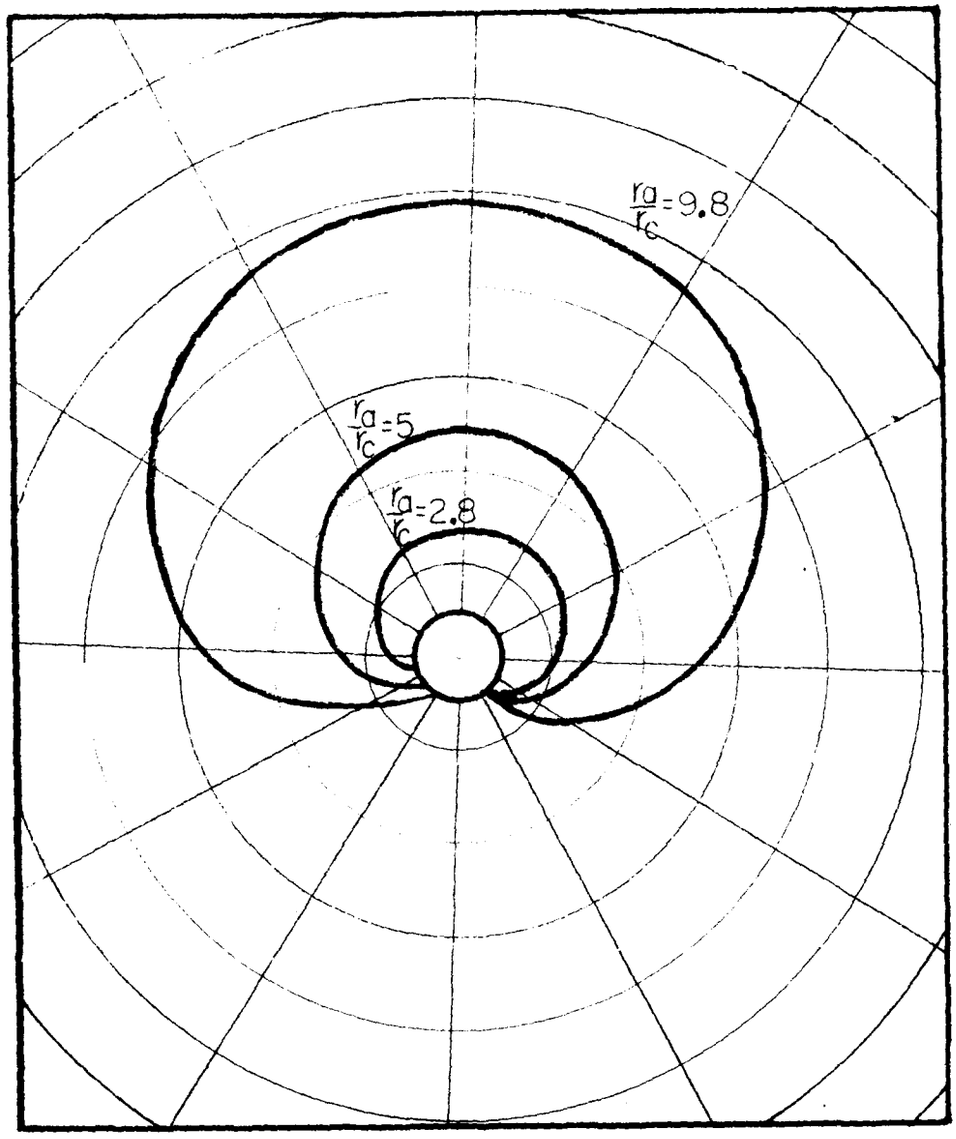

Figure 25

Electron trajectories for the static magnetron.

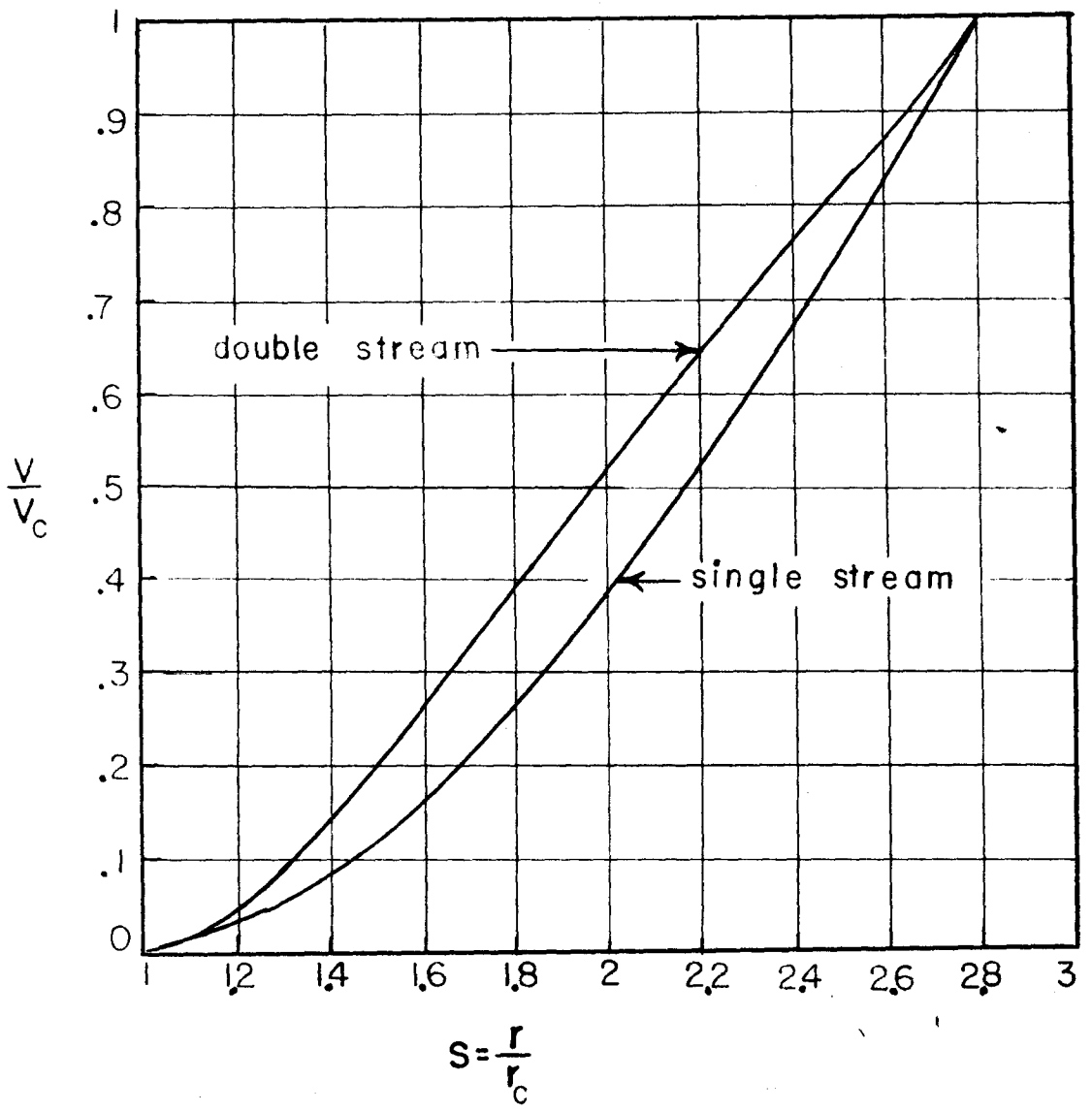

Figure 26

Voltage distribution in static magnetron at cut-off,

$r_a/r_c = 2.8$.

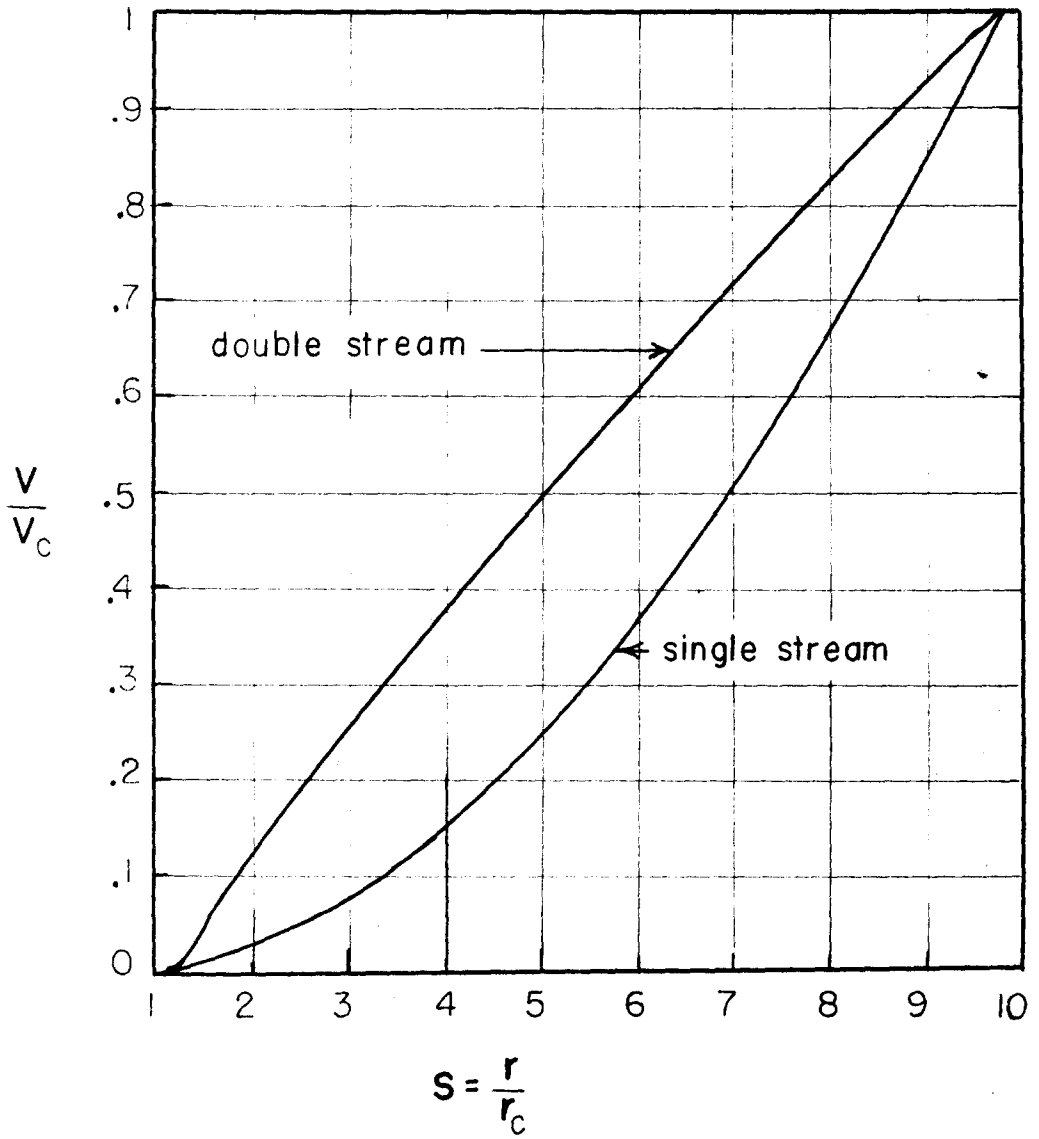

Figure 27

Voltage distribution in static magnetron at cut-off

$r_a/r_c = 9.8$.

APPENDIX II

RELATIVISTIC EFFECTS AND CUT-OFF

The relativistic effects occurring in an electrodynamical system such as the magnetron are completely accounted for by the change in the mass of a particle due to its velocity and by accounting for the electrical and magnetic fields of moving charged particles.[11] The change in the mass of the particle is accounted for by using the relation (127) between mass and velocity. The electrical and magnetic fields are accounted for by obtaining completely consistent solutions to Maxwell's equations.

Cut-off in the Absence of Space Charge in the Planar Magnetron

The assumption of no space charge effects makes the analysis applicable to the case of a single electron being released at the cathode, and allowed either to be captured at the anode or else to move out to a maximum distance from the cathode and then to return to the cathode. For this case, the force equations may be written as

$$f_x = d/dt(mv_x) = (-eB)\ dy/dt + e\ (dV/dx) \qquad (123)$$

$$f_y = d/dt\ (mv_y) = eB\ (dx/dt)\ . \qquad (124)$$

In these equations the mass must be considered as a function of velocity. The coordinates are taken as in Appendix I. Since space charge effects are neglected, B is independent of position and time; V is a function of position but not of time. With these conditions,

(124) can be integrated and becomes

$$mv_y = eBx \quad , \tag{125}$$

where it is assumed that the electron is released from the origin of coordinates with zero velocity. Substitution of this relation into (123) and integration yields

$$\frac{1}{2}\,(mv_x)^2 + \frac{1}{2}\,(eBx)^2 = e\int_o^t \frac{dV}{dx}\,(mv_x\,dt) \quad . \tag{126}$$

The relation between mass and velocity is

$$m = \frac{m_o}{\left(1 - u^2/c^2\right)^{\frac{1}{2}}} \quad , \tag{127}$$

where m_o = the rest mass of the electron;

u = total velocity of the electron ($u^2 = v_x^2 + v_y^2$)

c = velocity of light.

Alternatively, this equation can be written as

$$u^2 = c^2\,(1 - m_o^2/m^2) \quad . \tag{128}$$

The equation (126) for x velocity can be rewritten with the aid of (125) as

$$\frac{e}{m}\int_o^x m\,\frac{dV}{dx}\,dx = \frac{1}{2}\,m\,(v_x^2 + v_y^2) = \frac{1}{2}\,mu^2 \tag{129}$$

Substitution of (128) into (129) gives the result

$$\frac{1}{2}\,c^2\,(m^2 - m_o^2) = e\int_o^x m\,\frac{dV}{dx}\,dx \tag{130}$$

Differentiation of this equation with respect to x gives

$$c^2\, dm = e\, dV \quad . \tag{131}$$

This result is in accordance with the relativistic expression for kinetic energy, namely, the kinetic energy is the difference between the relativistic mass and the rest mass times the square of the velocity of light.[12] Equation (131) shows that there is a linear relation between mass and the voltage through which the charged particle has fallen. This is a special case of a more general proposition that, for point masses,

$$\text{kinetic energy} = c^2 (m - m_o) = \int_o^S F \cdot ds \ , \tag{132}$$

where F is the force on the point and ds is element of arc.

In the present case, the part of the force due to magnetic field does not contribute to the integral since it is perpendicular to the velocity so that $\int F \cdot ds$ equals eV. It is possible with the aid of the various proportionalities which have been derived to calculate a relativistic cut-off expression. First, it will be assumed that the x-velocity at the anode is zero. Equation (125) gives the y-velocity at the anode in terms of m if d is substituted for x. When this is substituted into equation (128), which relates mass and velocity, an equation relating m and B results. This is equivalent to a relation between B and V, which is the cut-off relation. For convenience,

the pertinent equations are listed.

$$v_y = eBd/m \quad ; \tag{133}$$

$$v_y^2 = c^2 (1 - m_o^2/m^2) \text{ , (since } v_x = 0) ; \tag{134}$$

$$c^2 (m - m_o) = eV \tag{135}$$

The cut-off relation is

$$\frac{2 e V_{cl}}{m_o c^2} + \frac{e^2 V_{cl}^2}{m_o^2 c^4} = \left(\frac{eBd}{m_o c}\right)^2 \tag{136}$$

where V_{cl} is the relativistic cut-off in the absence of space charge effects. To get an idea of the relativistic effect, equation (136) will be reduced to dimensionless variables. Let V_c be the cut-off voltage, neglecting all relativistic effects. Equation (76) gives V_c as $\frac{1}{2} (m_o/e) (e Bd/m_o)^2$.

Let γ_1 be defined as the ratio of the relativistic cut-off to the classical cut-off voltage

$$\gamma_1 = \frac{V_{cl}}{V_c} \tag{137}$$

Then from equation (136)

$$\gamma_1 \left(1 + \frac{eV_c}{2m_o c^2} \gamma_1\right) = 1 . \tag{138}$$

The subscript is used on γ_1 so that a similar notation may be used in the consideration of the same problem, including space charge effects. It is of interest that, while space charge did not affect the

calculations of the classical cut-off, there is a significant effect in the relativistic calculations.

The coefficient $\frac{1}{2}\ (e/m_o)\ c^2$ appearing in (138) is an absolute constant, the size of which determines the magnitude of the relativistic effect. This constant has a value

$$\frac{1}{2}\ (e/m_o)\ c^2 = 0.98 \times 10^{-6}\ \text{volts}^{-1} \qquad (139)$$

Figure 28 is a plot of γ_1 vs V_c. At $V_c = 5 \times 10^4$ volts, the relativistic cut-off is approximately 5% less than the classical cut-off.

Relativistic Cut-off in the Presence of Space Charge

A complete estimate of the relativistic effects on cut-off in the planar magnetron must include the effects of space charge. In order to set up a possible space charge condition in the planar magnetron, the classical results will be used as a guide. In the Brillouin steady state, it is supposed that the electronic motion is entirely parallel to the cathode surface, with zero velocity perpendicular to the cathode and anode surfaces. In order to maintain this motion, the force due to the electric field must exactly balance the force due to the magnetic field. Figure 29 shows the directions of the various velocity, field and force vectors in relation to each other and to the system of coordinates which is being used.

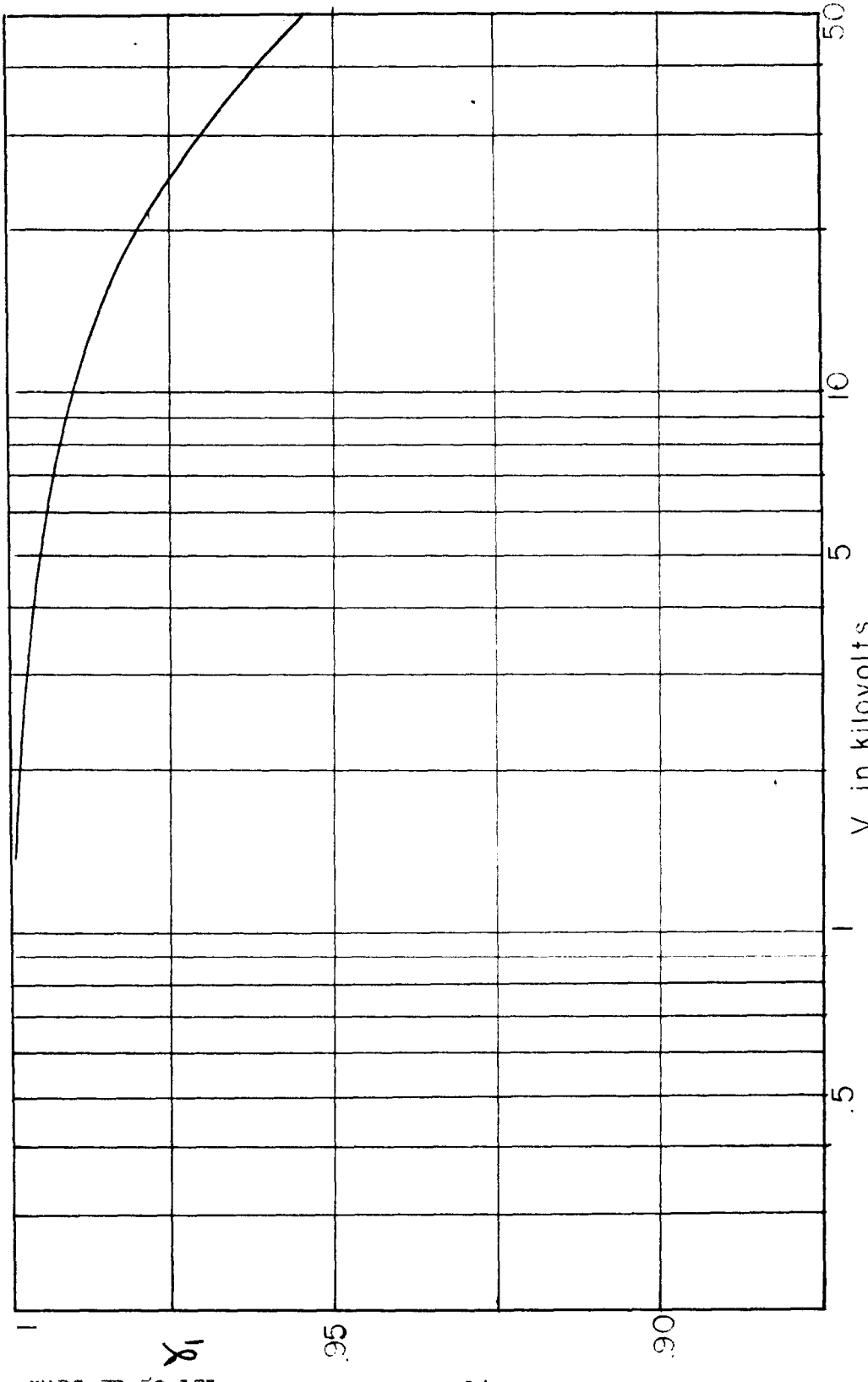

Figure 28
γ_1 as a function of V_c

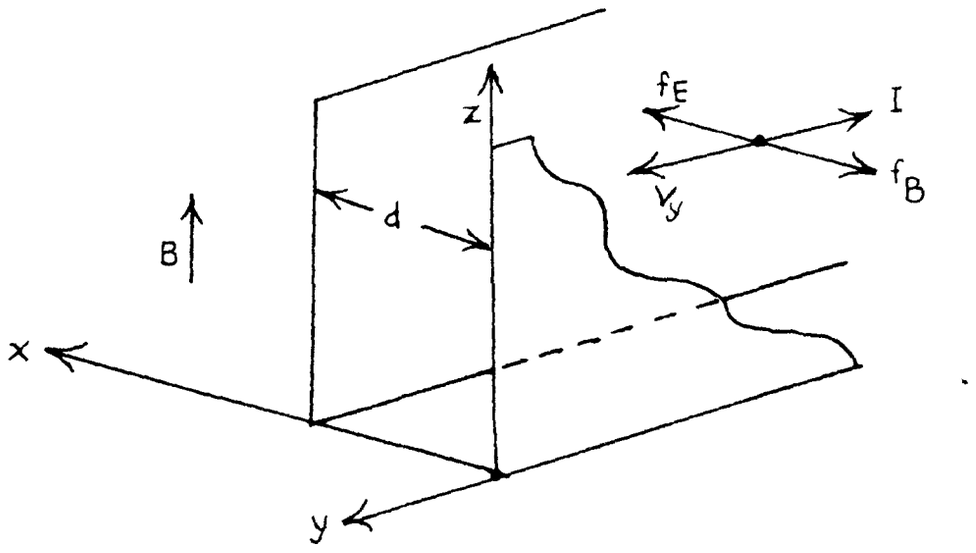

Figure 29

In the figure, f_E is the force associated with the electric field; f_B is the force associated with the magnetic field. The vector I is the current associated with the electronic motion with velocity v_y. It is seen that the effect of the magnetic field associated with I is to decrease the magnetic field at the cathode relative to the anode, or to increase the magnetic field at the anode relative to the cathode. Thus,

$$B = B_c - \mu \int_0^x J_y \, dx \quad , \tag{140}$$

where J_y is the y component of the current density vector; B_c is the magnetic field at the cathode. The permeability of free space is given by μ. Alternatively

$$B = B_a + \mu \int_x^d J_y \, dx \qquad (141)$$

where J_y and μ are as before and B_a is the magnetic field at the anode. In each case J_y is given by ρv_y, and since ρ is negative and v_y positive, J_y is negative (for the particular orientation of coordinates and field which have been chosen). The various equations which must be satisfied simultaneously include the divergence equation and the force equations (123) and (124), as well as equations (140) or (141) which give the variation of the magnetic field. The divergence equation is

$$\nabla \cdot D = \rho = - \epsilon (d^2V/dx^2) \qquad (142)$$

The further assumption of conservation of energy will be made. The relativistic statement of this is

$$(m - m_o) c^2 = eV \qquad (143)$$

For the condition of no current to the anode (assuming single stream), dx/dt must be zero and dy/dt independent of t. It is conceivable that there are other solutions where these conditions do not hold, and (formally at least) there is no anode current. Such solutions would be multiple velocity solutions and are discussed in a later section. As a consequence of the single stream conditions, the force on the electrons is zero. It follows from setting the force equal to zero that

$$eB\,(dy/dt) = e\,(dV/dx) \tag{144}$$

$$eB\,(dx/dt) = 0 \tag{145}$$

The law relating mass and velocity (Eq. 127) gives dy/dt in terms of mass m; equation (143) gives voltage in terms of mass. Substitution in (144) results in an equation which involves only the mass of the particle. From (128), with $u = v_y$

$$v_y^2 = c^2\,(1 - m_o^2/m^2)$$

and since from (131), $c^2\,d\,m = e\,dV$, (144) becomes

$$eBc\,(1 - m_o^2/m^2)^{\frac{1}{2}} = c^2\,dm/dx \tag{146}$$

where B is given by (140), (142), (131), and (127) as

$$B = B_c + \mu\epsilon \int_o^x \frac{c^2}{e}\,\frac{d^2m}{dx^2}\,c\,(1 - m_o^2/m^2)^{\frac{1}{2}}\,dx \tag{147}$$

or, from (141) as

$$B = B_a - \mu\epsilon \int_x^d \frac{c^2}{e}\,\frac{d^2m}{dx^2}\,c\,(1 - m_o^2/m^2)^{\frac{1}{2}}\,dx \tag{148}$$

Note that whichever expression is used for B

$$dB/dx = (c/e)\,(1 - m_o^2/m^2)^{\frac{1}{2}}\,(d^2m/dx^2) \tag{149}$$

where $1/c^2 = \mu\epsilon$.

Thus it is possible to obtain a differential equation which contains only m by solving (146) for B and differentiating. The

result is

$$\frac{dB}{dx} = \frac{c}{e} \frac{d}{dx} \frac{dm/dx}{(1 - m_o^2/m^2)^{1/2}} \tag{150}$$

$$(1 - m_o^2/m^2)^{1/2} (d^2m/dx^2) = \frac{d}{dx} \frac{dm/dx}{(1 - m_o^2/m^2)^{1/2}} \tag{151}$$

Equation (151) reduces to

$$m(d^2m/dx^2) = \frac{(dm/dx)^2}{1 - m_o^2/m^2} \tag{152}$$

This equation has the solution

$$m = m_o \cosh (\delta x + \sigma) \tag{153}$$

where δ and σ are constants of integrations.

Since $m = m_o$ at $x = 0$, $\sigma = 0$, so that

$$m = m_o \cosh \delta x . \tag{154}$$

The condition of space charge limitation is automatically taken care of since $dV/dx = c^2/e\,(dm/dx) = 0$ at $x = 0$. To evaluate δ, the conditions at the anode must be employed; thus

$$(m - m_o)\, c^2 = eV_a, \quad \text{at } x = d . \tag{155}$$

This results in

$$(m_o \cosh \delta d - m_o)\, c^2 = eV_a \tag{156}$$

or

$$\cosh \delta d = 1 + (eV_a)/(m_o c^2) . \tag{157}$$

The magnetic field B is obtained by substitution of (154) into (146)

$$B = \frac{(c/e)\ (dm/dx)}{(1 - m_o^2/m^2)^{1/2}} \tag{158}$$

or

$$B = (\ \delta\, cm_o/e) \cosh \delta\, x \tag{159}$$

$$B_c = \delta cm_o/e \tag{160}$$

$$B_a = (\ \delta\, cm_o/e) \cosh \delta\, d \tag{161}$$

Equations (160) and (161), together with (157) give the cut-off condition. For example, if it is assumed that the magnetic field at the anode is the same in the presence of space charge as in the absence of space charge, (161) and (157) give the relation between cut-off voltage and magnetic field in terms of the parameter δ.

The choice of boundary conditions for magnetic field depends on the way in which the current loop associated with the electron stream is closed. Thus, for cylindrical geometry, the field at the anode would be equal to the field in the absence of space charge since the anode is outside the current loop associated with the electron stream.

The relationship contained in (157) and (161) approaches the classical situation if $B_a \to 0$ (or $\delta \to 0$). Keeping terms of the order δ^2 in the expansion of (157) and (161), one obtains

$$1 + eV_a/m_o c^2 = 1 + \delta^2 d^2/2 \tag{162}$$

and

$$B_a = \delta\, cm_o/e \quad . \tag{163}$$

Elimination of δ from these equations gives the classical cut-off relation.

Let V_2 be the relativistic cut-off in the presence of space charge as derived on the basis of the extremely simple picture of parallel flow of electrons, with a single velocity function. The dimensionless ratio γ_2 is defined by

$$\gamma_2 = V_2/V_c = V_2/\left(\frac{1}{2} B_a^2 d^2 \frac{e}{m_o}\right) \tag{164}$$

In terms of γ_2 the parametric relations are

$$1 + \gamma_2 V_c e/(m_o c^2) = \cosh \delta d \tag{165}$$

$$\left[2V_c e/(m_o c^2)\right]^{1/2} = \delta d \cosh \delta d \tag{166}$$

The information contained in these equations is presented graphically in Fig. 30 with γ_2 plotted as a function of V_c. At V_c = 50 kv, the relativistic cut-off is 88% of the classical cut-off voltage. This compares to 95% for the case of no space charge.

The restriction to a single stream is a very serious one since it is known that (at least for non relativistic mechanics) a multiple stream can exist. The presence of space charge makes a significant difference in the calculated cut off, as has been seen. The existence of a possibility of a double stream was noted in the classical case as a consequence of the very simple calculation of the electron trajectories as based on an assumption of a single stream to the anode. This is not possible in the relativistic case because of the non-homogeneous nature of the problem. The

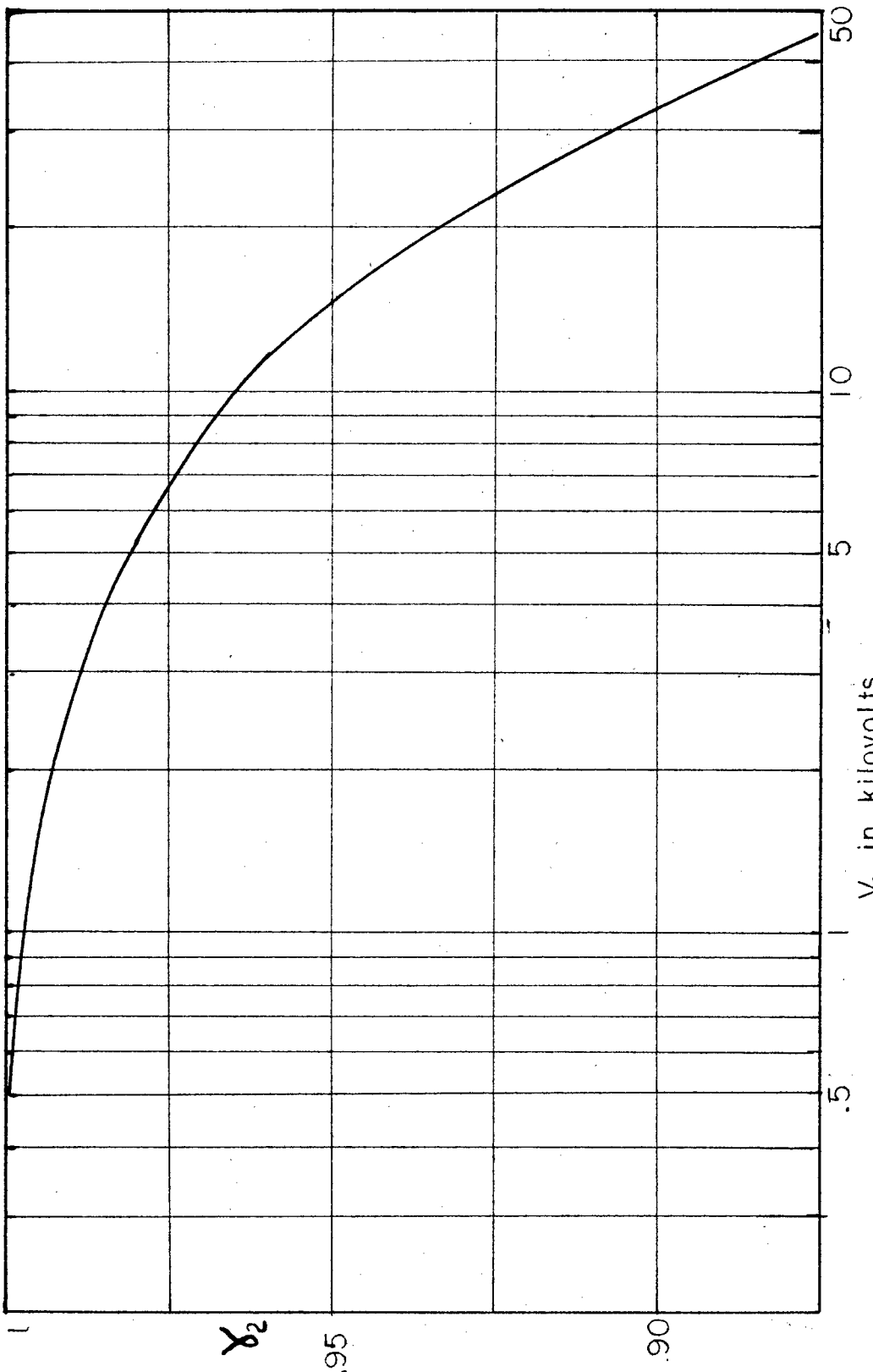

Figure 30

γ_2 as a function of V_c

effect that a double stream would have can be calculated easily to a first order of approximation since the magnetic field at moderately large voltages is the same whether a relativistic, or classical space charge solution is used. With this in mind, the magnetic field associated with a double stream of electrons will be calculated; the space charge density and velocity will be obtained from the classical calculations. Of course, these calculations are of significance only when the magnetic field of the stream is small compared to the static magnetic field. The voltage distribution and electron velocities will be taken as in equations (89) and (86), Appendix I. It will be assumed that there is zero net current to the anode, but that the electrons have velocities in the x direction. Current density and magnetic field will be calculated for this condition. The calculation is complicated by the transcendental nature of the equations defining the state. From Appendix I,

$$V = \frac{1}{2} \frac{m_o}{e} \left\{ \omega_o^2 x^2 + \frac{J_x^2}{\epsilon^2 \omega_o^2 B_o^2} (1 - \cos \omega_o t)^2 \right\} \qquad (167)$$

In these equations, B_o is used to indicate a zero approximation to B.

$$x = - \frac{J_x}{\epsilon \omega_o B_o} \left\{ t - \frac{1}{\omega_o} \sin \omega_o t \right\} \qquad (168)$$

$$dy/dt = eB_o x/m_o \qquad (169)$$

The equation relating x and t is bi-unique, but its transcendental nature does not allow solution for t in terms of x. The use of the equations implicitly will circumvent this difficulty. The x-velocity dx/dt is given by

$$\frac{dx}{dt} = - \frac{J_x}{\epsilon \omega_o B_o} (1 - \cos \omega_o t) . \qquad (170)$$

To calculate the space charge density, the procedure will be to follow an electron that leaves the cathode at t = 0, and calculate the space charge density along the trajectory at each time t. Using implicit differentiation, one obtains

$$\frac{dV}{dx} = \frac{m_o}{e} \left\{ \omega_o^2 x + \frac{- J_x}{\epsilon B_o} \sin \omega_o t \right\} \qquad (171)$$

$$\frac{d^2V}{dx^2} = \frac{m_o}{e} \omega_o^2 \left\{ \frac{1}{1 - \cos \omega_o t} \right\} \qquad (172)$$

The space charge density is given by

$$\rho = - \epsilon \frac{m_o}{e} \omega_o^2 \left\{ \frac{1}{1 - \cos \omega_o t} \right\} \qquad (173)$$

For the double stream of the hypothesis, in which there is a total current J_x (adding the absolute values of the densities in the two streams) and a net outward current of zero, the velocity must be zero at the anode or at x = d. This requires that J_x have certain discrete values, depending on the number of striations, or regions of infinite space charge density, between anode and cathode. The

magnetic induction of the electron stream is obtained by substitution into (140). The variable of integration x can be replaced with time t, integrating to the time which corresponds to the particular x plane. Thus

$$B = B_c - \mu \int_0^x J_y \, dx = B_c + \mu\epsilon \int_0^x \frac{m_o \omega_o^2}{e} \left\{ \frac{1}{1 - \cos \omega_o t} \right\} \frac{dy}{dt} \, dx,$$

$J_y \, dx = \rho \frac{dy}{dt} dx$ has been obtained from equations (173), (168), (169), and (170). The result is

$$B = B_c + \frac{\omega_o^2 B_o}{c^2} \left(\frac{- J_x}{\epsilon \omega_o B_o} \right)^2 \left[\frac{t^2}{2} + \frac{\cos \omega_o t}{\omega_o^2} \right]_0^t . \qquad (174)$$

The allowable discrete values of J_x are obtained from equations (96), (91) and (92). It is necessary that the transit angle be $2n\pi$ where n is an integer in order that the x velocity be zero at the anode. From equation (96)

$$\alpha = \frac{9}{4 n \pi} \qquad (175)$$

From (91), (92) and the classical cut-off relation (76)

$$J_x = - \frac{\epsilon}{n\pi} \sqrt{\frac{2e}{m_o}} \frac{V^{3/2}}{d^2}$$

$$J_x = - \frac{\epsilon}{n\pi} \frac{m_o}{e} \frac{\omega_o^3 \, d}{2} . \qquad (176)$$

When this value (eq. 176) is substituted into equation (174), the result is

$$B = B_c + \frac{d^2 B_o^3 e^2/m_o^2}{4 n^2 \pi^2 c^2} \left[\frac{(\omega_o t)^2}{2} + \cos \omega_o t \right]_o^t \qquad (177)$$

This equation defines the first approximation to B at the x plane. To find the total effect on the field, the value of t at the anode must be used. This value is $\omega_o t = 2n\pi$. This substitution yields

$$B_a = B_c + \frac{e^2 B_o^3 d^2}{2m_o^2 c^2} \qquad (178)$$

If δd is assumed small, in equations (157), (160) and (161), and if expansions are used for the functions, the same relation between B_a and B_c may be obtained. Thus, to the first approximation, the total reduction of the field at the cathode is the same for the single stream as for the double stream configuration. The details, however, are different. In each case

$$B = B_c + B_o \frac{eV_c}{m_o c^2} f(x/d) \qquad (179)$$

For the single stream, expansions of equations (157), (159), (160), and (161) retaining only terms of the order δ^2 results in

$$f\left(\frac{x}{d}\right) = \left(\frac{x}{d}\right)^2 . \qquad (180)$$

For the double stream, f (x/d) is an implicit function of (x/d) and is obtained from the cut-off relation (76), and equations (168), (176), and (177). This implicit relation is

$$\frac{x}{d} = \frac{1}{2n\pi} (\theta - \sin\theta)$$

$$f(x/d) = \frac{(\theta^2/2) + (\cos\theta - 1)}{2\pi^2 n^2} \qquad (181)$$

Figure 31 is a plot of the functions of x/d for the single stream case, and for the double stream case with n = 1.

To carry the approximation further, it will be assumed that B(x) is given by a function as in (179), which will be used to re-calculate the electron orbits. The relativistic expression for the y velocity is

$$dy/dt = e/m \int_0^x B\,dx \qquad (182)$$

For the cut-off condition v_x is zero at the anode so that

$$u = dy/dt = e/m \int_0^d B\,dx = c\,(1 - m_o^2/m^2)^{1/2} \qquad (183)$$

Use of the relation (143) between m and V results in

$$V + \frac{eV^2}{2m_o c^2} = \frac{e}{2m_o} \left[\int_0^d B\,dx\right]^2 . \qquad (184)$$

It will be assumed that the magnetic field at the anode is the same as the field in the absence of space charge. With this assumption, (178) and (76) may be used to express (179) as

$$B = B_o \left\{ 1 - \frac{eV_c}{m_o c^2} + \frac{eV_c}{m_o c^2} f\left(\frac{x}{d}\right) \right\} \qquad (179a)$$

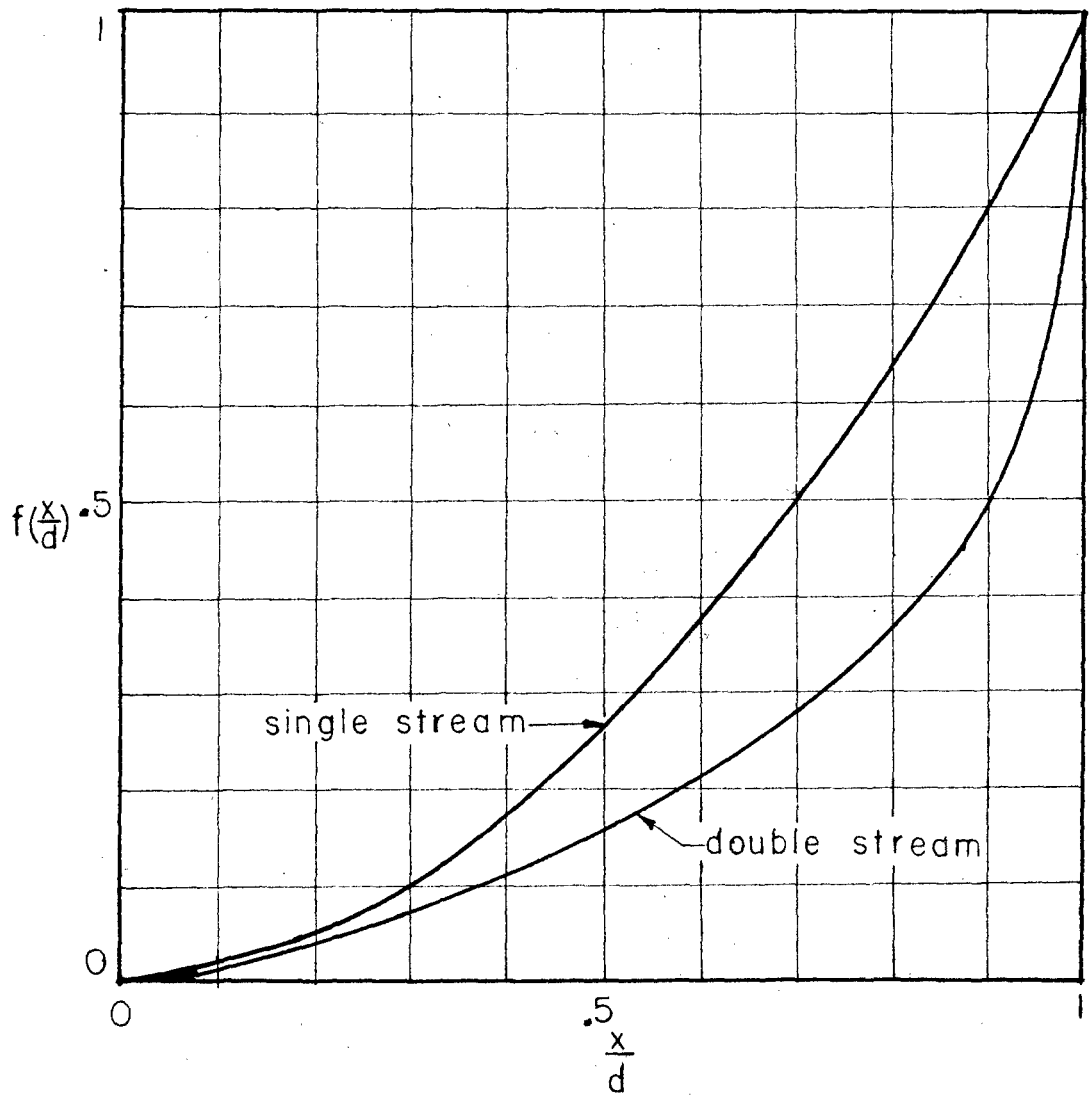

Figure 31

Substitution of this general form for the variation of B (179a) into equation (184) yields the general form of the cut-off relation. The result is

$$V + \frac{eV^2}{2m_o c^2} = V_c \left[1 - \frac{eV_c}{m_o c^2} + \frac{eV_c}{m_o c^2} \int_o^1 f\left(\frac{x}{d}\right) d\left(\frac{x}{d}\right) \right]^2 \quad (185)$$

For the special case of a single stream, from (180) $f(x/d) = (x/d)^2$, and the cut-off relation is

$$V + \frac{eV^2}{2m_o c^2} = V_c \left[1 - \frac{2}{3} \frac{e V_c}{m_o c^2} \right]^2 . \quad (186)$$

For the case of the double stream, the integral can be calculated graphically. For the case of only one striation, it is equal to approximately 1/5. This results in the cut-off relation

$$V + \frac{eV^2}{2m_o c^2} = V_c \left[1 - \frac{4}{5} \frac{eV_c}{m_o c^2} \right]^2 \quad (187)$$

Let $\gamma_2 = V/V_c$ for the single stream calculation and $\gamma_2^* = V/V_c$ for the double stream calculation. The cut-off equations become

$$\gamma_2 \left[1 + \frac{V_c}{10^6} \gamma_2 \right] = \left[1 - \frac{4}{3} \frac{V_c}{10^6} \right]^2 \quad (188)$$

and

$$\gamma_2^* \left[1 + \frac{V_c}{10^6} \gamma_2^* \right] = \left[1 - \frac{8}{5} \frac{V_c}{10^6} \right]^2 . \quad (189)$$

The variables γ_2 and γ_2^* are shown as functions of V_c in figure 32.

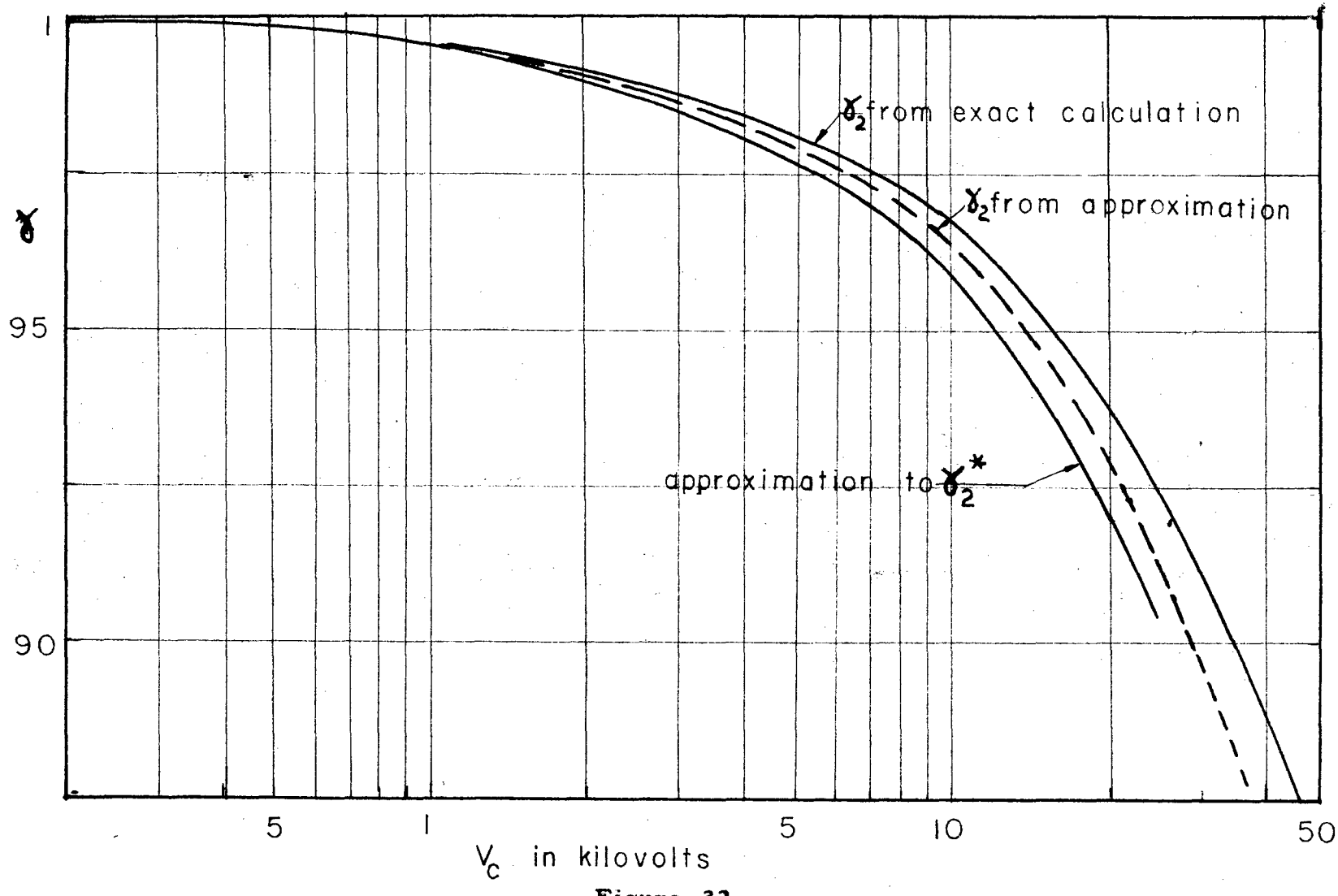

Figure 32

γ_2^* and γ_2 as a function of V_c

The use of the classical solution for space charge density and velocity to calculate the z magnetic field neglects effects of the order $(eV_c/m_oc^2)^2$. This is less than 1% for voltages up to 50 kv. Figure 32 shows the effect of the approximation for the single stream case. The exact plot of γ_2 is included for reference.

Cylindrical Geometry

The pertinent algebraic equations embodying the space charge effects, magnetic effects, conservation of charge, etc., for cylindrical geometry are listed:

$$\frac{\partial D_r}{\partial r} + \frac{1}{r} D_r = \rho \tag{190}$$

$$\frac{\partial H_z}{\partial r} = - \rho r \frac{d\phi}{dt} \tag{191}$$

These equations are the divergence and curl equations for electric and magnetic fields, respectively, from macroscopic electromagnetics.

$$\frac{d}{dt}\left(m \frac{dr}{dt}\right) - mr\left(\frac{d\phi}{dt}\right)^2 = e \frac{dV}{dr} - B_z er \frac{d\phi}{dt} \tag{192}$$

$$\frac{d}{dt}\left(mr^2 \frac{d\phi}{dt}\right) = erB_z \frac{dr}{dt} \quad . \tag{193}$$

These equations are the relativistic equations of motion of an electron with charge -e in cylindrical coordinates.

$$(m - m_o) c^2 = eV \tag{194}$$

$$m = \frac{m_o}{(1 - u^2/c^2)^{1/2}} \tag{195}$$

$$u^2 = c^2 (1 - m_o^2/m^2) \quad . \tag{196}$$

These equations are the relativistic statements of the relations between mass, velocity (u) and kinetic energy. As a first approximation to a solution, it will be assumed that B_z is a constant equal to B_o, the magnetic field in the absence of space charge. This allows calculation of the trajectories to get an estimate of B_z. Recalculation of the electron trajectories should give a close estimate of cut-off for moderate voltages. The initial calculation of the trajectories will give the cut-off in the absence of space charge effects. Integration of (193) with the assumption of $B_z = B_o$, a constant, results in

$$\frac{d\phi}{dt} = \frac{B_o e}{2m} (1 - r_c^2/r^2) \quad . \tag{197}$$

When this result is substituted into equation (192), this equation can be integrated, and the result is

$$\frac{1}{2}\left(m \frac{dr}{dt}\right)^2 + \frac{B_o^2 e^2}{4}\left(\frac{r^2 - r_c^2}{2} + \frac{r_c^4}{2r^2} - \frac{r_c^2}{2}\right) = \frac{e^2 V^2}{2c^2} + m_o eV \quad . \tag{198}$$

This equation was obtained without knowledge of the variation of V; it depends only on its value at the limits of the integration. To obtain the cut-off condition, set $dr/dt = 0$ at $r = r_a$. The result

is

$$V\left(1 + \frac{eV}{2m_o c^2}\right) = \frac{B_o^2 e r_a^2}{8 m_o}\left(1 - \frac{r_c^2}{r_a^2}\right)^2 \qquad (199)$$

The low voltage limit of this expression is the Hull cut-off formula and is

$$V_c = \frac{B_o e r_a^2}{8 m_o}\left(1 - \frac{r_c^2}{r_a^2}\right)^2 \qquad (200)$$

Re-expression of the relativistic cut-off equation (199) in terms of the dimensionless parameter $\gamma_1 = V/V_c$ gives

$$\gamma_1\left(1 + \frac{eV_c}{2m_o c^2}\,\gamma_1\right) = 1 \quad . \qquad (201)$$

This is the cut-off relation in the absence of space charge effects; it is identical to (138) which is the analogous relation for planar geometry. To obtain an estimate of the magnetic effect of the electron stream, an estimate of space charge density must be obtained. It will be assumed that the electrons move around the cathode in circular orbits with the forces just balanced out. A completely consistent solution was obtained in the analogous situation for the planar case. If the same techniques are tried for the cylindrical case, a singular differential equation is encountered. The type of singularity makes this equation very difficult to handle. However, effects on the magnetic field of the order of $eV/m_o c^2$ can be calculated using the classical space charge density and velocity.

Thus, assuming $dr/dt = 0$, $d\phi/dt$ is given by equation (197); V is given by (200) where the general radius r is substituted for r_a. Thus

$$V = \frac{B_o^2 e r^2}{8 m_o} \left(1 - \frac{r_c^2}{r^2}\right)^2 \quad . \tag{202}$$

Substituting into equation (190) for D_r gives the space charge density as

$$\rho = - \frac{\epsilon}{8} B_o^2 \frac{e}{m_o} \left(4 + 4 \frac{r_c^4}{r^4}\right) \quad . \tag{203}$$

Variation in magnetic field is given by

$$\frac{dB_z}{dr} = - \mu \rho r \frac{d\phi}{dt} \quad . \tag{204}$$

This is easily integrated, and gives

$$B_z = B_c + \frac{B_o^3 e^2}{4 m_o^2 c^2} \left\{ \frac{r^2}{2} - \frac{r_c^2}{4} - \frac{r_c^4}{2r^2} + \frac{r_c^6}{4r^4} - r_c^2 \ln \frac{r}{r_c} \right\} \tag{205}$$

Use of this value of B_z in equation (193) to find the first order effects on velocity will make possible the calculation of first order effects on cut-off voltage. Thus

$$mr^2 \frac{d\phi}{dt} = e \int_{r_c}^{r} r B_z \, dr$$

$$= e \int_{r_c}^{r} \left\{ B_c r + \frac{B_o^3 e^2}{4 m^2 c^2} \left(\frac{r^3}{2} - \frac{r r_c^2}{4} - \frac{r_c^4}{2r} + \frac{r_c^6}{4r^3} - r r_c^2 \ln \frac{r}{r_c} \right) \right\} dr \quad . \tag{206}$$

The integration yields

$$mr^2 \frac{d\phi}{dt} = e\left\{\frac{B_c}{2}(r^2 - r_c^2) + \frac{B_o^3 e^2}{4m^2c^2}\left(\frac{r^4}{8} - \frac{r_c^4}{8} + \frac{r^2 r_c^2}{8} - \frac{r_c^6}{8r^2} - \frac{r_c^4 + r^2 r_c^2}{2} \ln \frac{r}{r_c}\right)\right\}. \quad (207)$$

If it is assumed that the magnetic field at the anode is the same as the field in the absence of space charge, thereby eliminating B_c from equation (207), (207) becomes

$$mr_a^2 \frac{d\phi}{dt} = e\left\{\frac{B_o}{2}(r_a^2 - r_c^2) - \frac{B_o^3 e^2}{8m^2c^2}\left(\frac{r_a^4}{4} - r_a^2 r_c^2 + \frac{r_c^6}{r_a^2} - \frac{r_c^8}{4 r_a^4} + 2r_c^4 \ln \frac{r_a}{r_c}\right)\right\}. \quad (208)$$

The cut-off relation is obtained by substitution into equations (194) and (196) relating mass, velocity and voltage. Let $k = r_a/r_c$; the resulting relation may be written as

$$\frac{V}{V_c}\left(1 + \frac{eV_c}{2m_oc^2}\frac{V}{V_c}\right) = \left\{1 - \frac{eV_c}{2m_oc^2} g(k)\right\}^2 . \quad (209)$$

where

$$g(k) = \frac{4 - 4k^4 + k^6 - 1/k^2 + 8k^2 \ln k}{(k^2 - 1)^3} . \quad (210)$$

As a check on the result, we note that the limit of $g(k)$ as $k \to 1$ is 4/3, resulting in the cut-off condition as in the planar case. The function $g(k)$ is shown in Fig. 33. Since $g(k)$ stays at a value near 1, the reduction in cut-off voltage due to relativistic

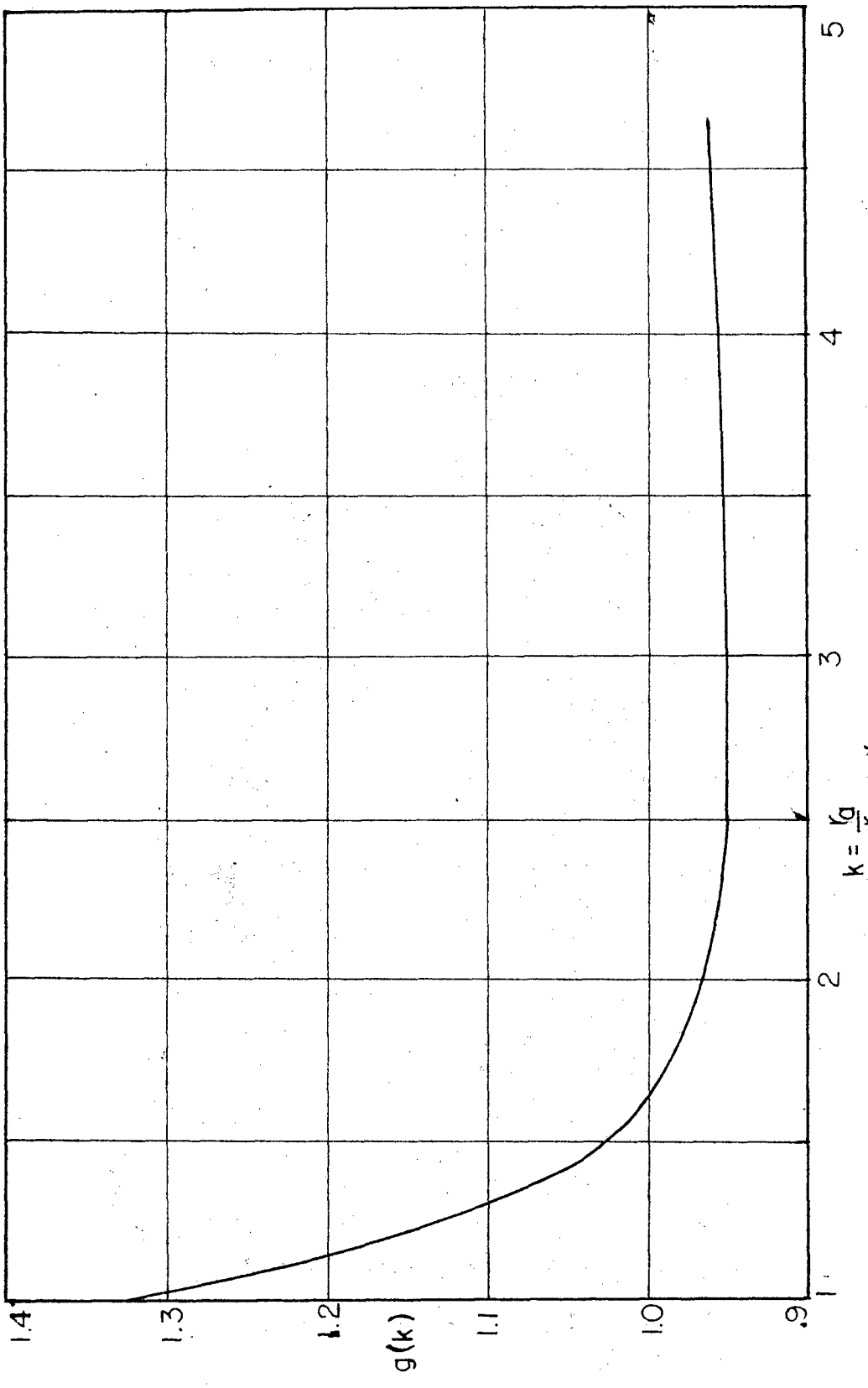

Figure 33

effects is of the same order of magnitude for cylindrical geometry as for planar geometry. This effect is of the order of 15% reduction in cut-off voltage when the classical cut-off voltage is 50 KV.

BIBLIOGRAPHY

(1) Collins, G.B., Microwave Magnetrons, New York. McGraw-Hill Book Co., 1948, pp. 98-99.

(2) Bell Laboratories Staff, Radar Systems and Components, New York: D. Van Nostrand Co., 1949, pp. 116-120.

(3) Willshaw, E.E., and Robertshaw, R.G., "Behavior of Multiple Circuit Magnetrons in the Neighborhood of the Critical Anode Voltage," Proc. Phys. Soc. B, 63, (Jan. 1950), pp. 41-45.

(4) Jepsen, R.L., "Enchanced Emission from Magnetron Cathodes," A doctoral thesis presented to Columbia University

(5) Welch, H.W., and Dow, W.G., "Analysis of Synchronous Conditions in the Cylindrical Magnetron Space Charge," J. Appl. Phys. 22, (April 1951), pp. 433-38.

(6) Slater, J.C., Microwave Electronics, New York: D. Van Nostrand Co., 1950.

(7) Marton, L., Advances in Electronics III, Section X (L. Brillouin) New York: Academic Press, Inc., 1951.

(8) Slater, J.C., op. cit.

(9) Marton, L., op. cit.

(10) Jepsen, R. L., op. cit.

(11) Tolman, R.C., Relativity, Thermodynamics and Cosmology, Oxford: At the Clarendon Press, 1934.

(12) Tolman, R.C., op. cit.